FORROST: Advances in On-Orbit Robotic Technologies

R. Lampariello[1], N. W. Oumer[1], J. Artigas[1], W. Rackl[1], G. Panin[1], R. Purschke[2], J. Harder[2], U. Walter[2], J. Frickel[3], I. Masic[4], K. Ravandoor[5], J. Sch arnagl[5], K. Schilling[5], K. Landzettel[1], G. Hirzinger[1]
[1]Robotics and Mechatronics Center (DLR), 82234 Weßling, Germany, email: *roberto.lampariello@dlr.de*
[2]Institute of Astronautics (LRT), 85748 Garching, Germany, email: *j.harder@tum.de*
[3]LIKE (FAU), 91058 Erlangen, Am Wolfsmantel 33, Germany, email: *juergen.frickel@fau.de*
[4]SpaceTech GmbH, 88090 Immenstaad am Bodensee, Germany, email: *ismar.masic@spacetech-i.com*
[5]University of Würzburg, Chair for Computer Science VII, Am Hubland 97074, Germany, email: *ravandoor@informatik.uni-wuerzburg.de*

***Abstract*—Orbital robotics is receiving growing attention worldwide for applications in servicing and repositioning of partially or fully defective satellites. In this paper, we present the scope and main results of a four-year research project, which aimed at developing necessary robotic technologies for such applications. The scope is two-fold, since we address both the human-operated robotic operational mode, referred to in robotics as force-feedback teleoperation, as well as the alternative autonomous mode, for the specific task of approaching and grasping a free-tumbling target satellite. We present methodological developments and experimental as well as numerical validations in the fields of tele-communications, computer vision, robot and spacecraft control and system identification. The results of this work constitute important advances in the fundamental building blocks necessary for the orbital applications of interest.**

TABLE OF CONTENTS

1. INTRODUCTION

Attempts nowadays to increase the maturity of orbital space systems aim at technological developments which allow their disposal, in case of irreparable failure, or their routine servicing, in case of partial failure or necessity of an upgrade. While the disposal task is the end goal of Active Debris Removal (ADR), a discipline of steadily increasing importance, the capacity to perform On-Orbit Servicing (OOS) tasks has undoubtedly always been an attractive prospect. In this paper, we describe the outcomes of a four-year project, FORROST, which involved different parties all located in the German state of Bavaria, and which focused on the development of key robotic technologies to eventually make the tasks above technically feasible.

The first and most relevant problem, in view of both ADR and OOS, is that of grasping and stabilizing a non-cooperative tumbling target object (e.g., a defective satellite), referred to here as Target, by means of a robot manipulator mounted on a satellite, referred to here as Servicer (see Fig. 1). Non-cooperative relates both to the fact that the Target is uncontrollable and that it does not present any design features which support its grasping. The task as such is novel, since in all previously flown missions to date (e.g., ETS-VII, Orbital Express) [1], the Target was cooperative. Existing programs around the world are addressing this particular task extensively: see, for example, DEOS in Germany, eDeorbit at ESA, or Phoenix in the USA.

The specific research work conducted within FORROST addressed different aspects related to the grasping task described above. These involve two principal robotic operational modes: the teleoperation and the semi-autonomous mode. In the first, an operator on ground controls the robot through a force-reflecting input device to execute the task, with the aid of sensor signals from the on-board cameras. In the second, an algorithm on ground computes a feasible and time-synchronized trajectory for the robot, which is then fed to the on-board closed-loop controller for execution. Both these approaches can be argued to have their own strengths, or may even be seen as complementary in a shared-autonomy setting. This subject however, is not addressed here. Instead, some of the fundamental functionalities for their realization are addressed in some detail.

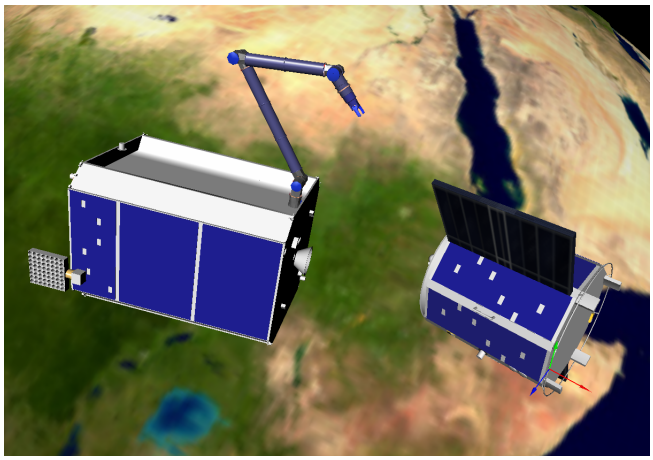

Figure 1: FORROST orbital scenario: Servicer satellite with kinematically redundant robot manipulator (left) and tumbling Target satellite (right). Coordinate frame of predefined grasping point on Target shown.

978-1-4799-5380-6/15/$31.00

We begin with the robotic teleoperational mode. The contribution here involves the development of an efficient communication link between the ground station and the robot in orbit, through a relay geostationary satellite. The gained efficiency has the particular benefit of minimizing the time-delay which is introduced in the robot's dedicated control loop, thus providing a potential effectiveness of force-feedback in the context of robot teleoperation. First, experimental results are described with a real geostationary satellite and a simple robotic system.

We then address the development of robot and spacecraft control methods to support the autonomous operational mode. A dedicated motion planner provides a feasible reference trajectory, based on a simulation model of the environment and on a motion prediction of the tumbling motion of the Target. The on-board robot feedback controller is then responsible for tracking the reference trajectory, while accounting for modelling and prediction errors. The free-floating dynamics of the robot, resulting from the fact that the carrying Servicer satellite is not actuated during the grasping phase, is accounted for. This operational strategy is also supported by new system identification and satellite collision detection and avoidance capabilities.

In Section 4 computer vision is addressed. In particular, two different approaches for the specific task of determining motion estimates of the tumbling Target from on-orbit measurements of a camera system are first described. The motion estimates are necessary for the generation of the Target motion prediction, which aids the generation of a reference trajectory for the grasping task, as well as for the collision avoidance tasks. Both a stereo vision system and a PMD (Photonic Mixer Device) camera were investigated. The developed methods are based on the knowledge of a geometric model of the Target, assumed to be given. Both hardware approaches were validated with experimental data, generated with two different experimental facilities at the German Aerospace Center (DLR) and at the University of Wuerzburg. A further means of validation was analyzed, which consisted in the generation of visual camera images by means of computer rendering techniques. These allow us to reproduce different lighting conditions, material reflective properties, camera lens parameters and target motion parameters.

2. Research Scope of FORROST

In this Section the chosen scenario, as well as the two robot operational modes of interest are briefly introduced.

Operational Scenario

The operational scenario is depicted schematically in Fig. 2. Of notice is the fact that the Target is assumed to be in a Low Earth Orbit and commanded through a communication link via a geostationary satellite. The principal actors (see also Fig. 1) are the Servicer, a fully controllable satellite which also carries a robot manipulator, the Target and the human operator at the Ground Station.

A further aspect which describes the scenario of interest is the geometry and assumed motion of the Target. The first is such that solar panels may be present, to represent realistic conditions and control challenges, with respect to collision avoidance. The second is such that the assumed tumbling motion may be reduced to a flat spin (a pure rotation about a fixed inertial axis), but that the orientation of the rotation axis

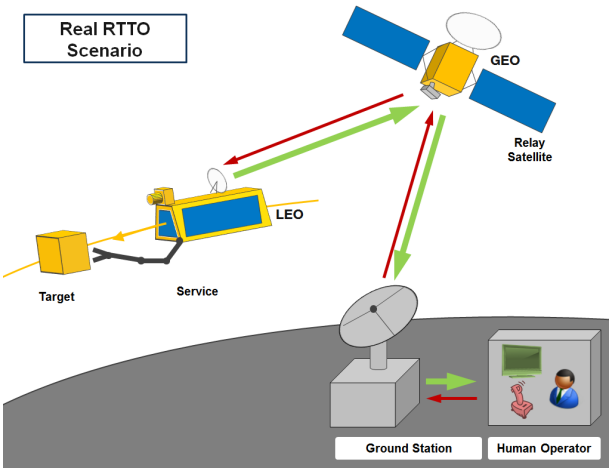

Figure 2: FORROST Real-Time Teleoperated (RTTO) Scenario.

may be general.

The main task of interest is the grasping (to include the stabilization) of the Target by means of the robot manipulator on the Servicer. The latter is not controlled in its attitude or position during the execution of the grasping task. As such, a free-floating dynamics results for the robot [1].

On-board manipulation is also relevant to the developments herein, in particular in relation to the implementation of the teleoperation mode. In this setting, the operator on ground may provide necessary intelligence which is otherwise difficult to achieve. The force-reflective property intrinsic to telepresence is argued here to provide enhanced capabilities for an operator on ground who operates on a remote environment. This property is however strongly dependent on the time latency in the communication system in play.

Robotic Operational Modes

The teleoperation and semi-autonomous operational modes are presented conceptually in Fig.3. It is evident that the communication link between the ground station and the robot plays a fundamental role, due to the necessary distribution of the computational resources between on-ground and on-board, as well as due to the interplay between the actors involved.

3. Teleoperation Through Geostationary Satellites

In space teleoperation, the user controls a space robot through a haptic device located on ground. The low-level real-time control actions are distributed between the robot itself and the haptic device. To that end, the kernel of the teleoperation mode contains a bilateral controller, whose primary goal is to guarantee stable performance of the force-feedback control loop under a set of communication characteristics. The topic of space teleoperation has been a matter of controversy, mainly arising from an established belief that communication time delays resulting from space links unavoidably jeopardize any teleoperation possibility. The main difficulty is to achieve a real-time communication infrastructure capable of long lasting communication windows while keeping moderate delays. The point-to-point paradigm was first presented during the

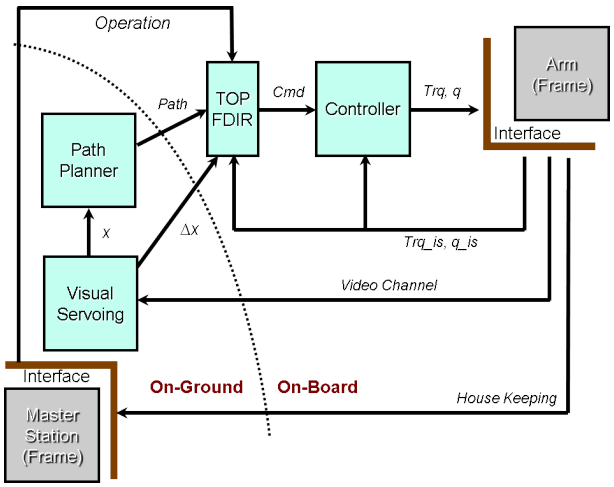

(a)

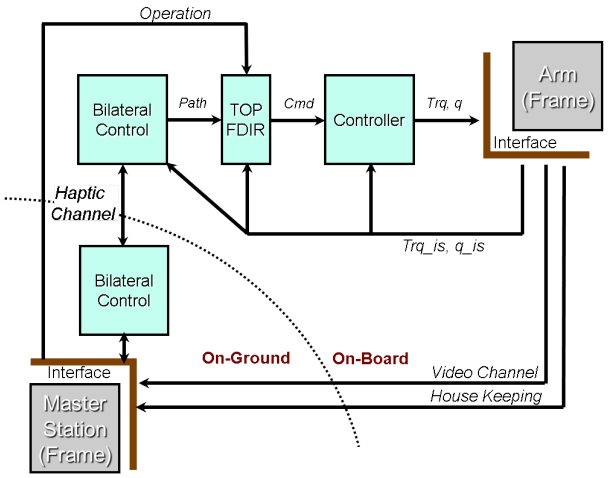

(b)

Figure 3: Functional block-diagram for (a) teleoperation and (b) autonomous operational modes. Primary software elements shown in green. The TOP/FDIR block represents an on-board task control and monitoring functionality.

ROKVISS experiment [2], where high performance teleoperation could be achieved with relative ease due to the resulting low time delays (around 20 ms) and low jitter. The used infrastructure allowed fast (500 Hz) real-time communication between the DLR, close to Munich, and the ISS Russian module. However, the ISS overflight communication windows allowed sessions of 5 to 10 minutes.

Feasibility of true real-time communication space links is a subject of interest among the space and robotics industry. Discussions on the robot control requirements and possibilities offered by existing and future communication infrastructures are currently underway. Robot control engineers set requirements on maximum allowed time delays and jitters, according to performance goals and stability criteria for the given system. In the following section we present a real-time communication link on the base of the ASTRA satellite that meets such requirements, that is, for implementing a force-feedback teleoperation system.

In FORROST, a unique communication link based on the Astra GEO-Satellite (presented later in this Section) was tested. This link is representative of a GEO-Relay infrastructure, where an on-ground haptic device and space robot are linked via a GEO satellite. In general, GEO relay infrastructures can achieve uninterrupted streams that span up to 1 hour [3]. On the downside, communication delays increase dramatically.

Fundamental questions are addressed in this article that deal with the feasibility of force-feedback based teleoperation using GEO relay infrastructure include the following:

- How large is the time delay resulting from the GEO space link?
- How strong is the jitter effect between data packages?
- Under these circumstances, is teleoperation with force-feedback still possible?

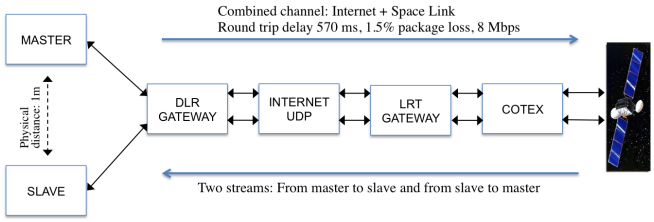

Figure 4: Bilateral Controller communication structure. The arrow heads indicate the bilateral character of the system.

Fig. 4 shows a high level scheme of the proposed setup along with its main characteristics. The factors affecting the stability and performance of the (bilateral) control closed-loop can be divided into constant and variable time delay, jitter and packet loss. Many approaches have been proposed since as early as the 1980's, but only a few succeed in coping with these three factors simultaneously. For instance, a constant time delay assumption cannot be made in the type of communications addressed in this paper. If furthermore stability depends on such an assumption, system damages might occur. Note that these factors are specially critical for the haptic channel (force-feedback loop) due to their destabilizing effects. Other perceptual modalities such as provided by the visual channel can tolerate higher delays, jitters and packet losses without compromising stability, as they are not involved in a low-level control loop; that is, performance might be affected, but not stability in terms of control. The approach used to compensate for these destabilizing effects is based on the Time Domain Passivity [4] and Time Delay Power Networks (TDPN) framework [5], [6]. This framework allows us to design bilateral control structures with arbitrary architectures, e.g. Position-Force, Position-Position or 4-Channels [7], while guaranteeing stability under any of the above communication aspects.

Teleoperation Experiments using a GEO Link

The system described in Fig. 4, along with the ASTRA-based space link, was implemented to test the performance of the teleoperation system. Details on the space link are provided further down in this Section.

Master and slave devices consisted of a pair of single degree-of-freedom (d.o.f.) devices. Such devices fit very well in experiments of this sort since they allow us to focus on pure bilateral control rationale, that is, disregarding classical topics related to non-linearities, multi-body dynamics, etc., that are irrelevant for the purposes of the test. Fig. 5 shows one of these devices [8].

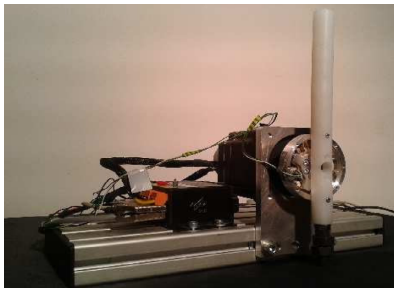

Figure 5: 1 d.o.f. device consisting of brushless motor, a force-torque sensor and a real-time control interface at 1000Hz

The performance of the communication link obtained from the DLR, located in Oberpfaffenhofen (Germany) and the ASTRA W3L is shown in Fig. 6. Note that this link presents two segments with different characteristics: a standard UDP segment through the Internet, between the DLR and the LRT (located in Garching, Germany); and a space segment, from the LRT to the satellite. The measured round-trip delay (i.e., one way up to GEO satellite - one way down to Ground station) due to the physical data transmission of the space segment was on average 260 ms. The delay introduced by the UDP link kept below 10 ms. Note that the DLR and the LRT are geographically very close.

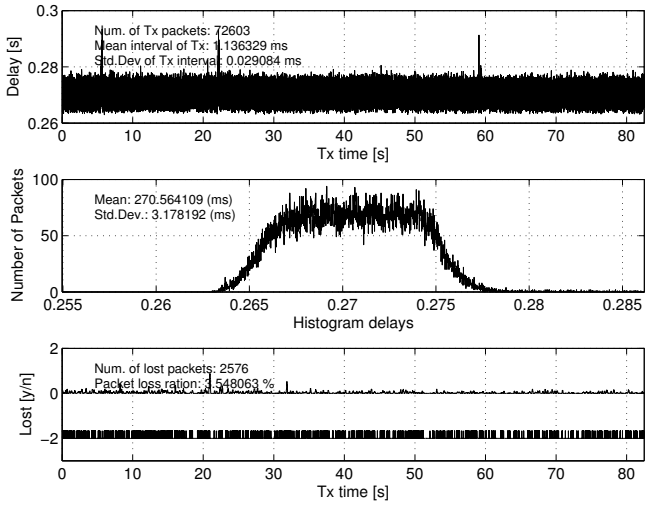

Figure 6: Delay and Jitter measurements considering the complete setup described in Fig. 4

Two experiments are highlighted:

Teleoperation with Force-feedback Through the Combined Space and UDP Link—where the system described in Fig. 4 was implemented with the obtained link performance, shown in Fig. 6. As can be seen, the link included one forward path, from the DLR to the ASTRA satellite, and back. Fig. 7 shows both the position tracking and a clear force-reflection.

Teleoperation with Force-feedback Through the Combined Space and UDP Link and GEO-Relay Simulation—Fig. 8 shows the obtained performance of the communication link described with an added conservative constant time delay of 300 ms. This setup is representative of GEO-Relay based

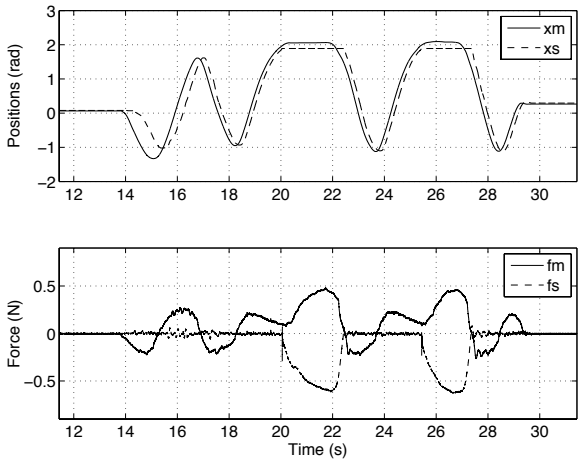

Figure 7: Performance of the haptic channel with the combined UDP / space link (Mean delay 270ms). xm = master position; xf = slave position; fm = master force; fs slave force

infrastructures, where two complete round trips must be considered. Again, the two main control objectives, position tracking and force reflection are achieved. Table 1 shows a summary of the involved time delays in this setup.

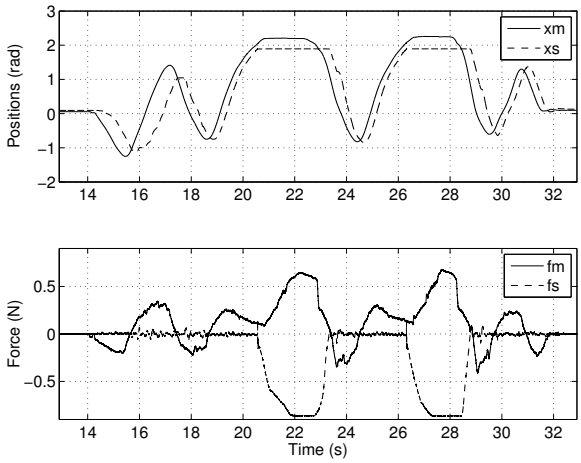

Figure 8: Performance of the haptic channel with the combined UDP / space link and simulated GEO-Relay (Mean delay 570ms). xm = saster position; xf = slave position; fm = master force; fs slave force

Table 1: **Summary of time delay values**

Delay Type	**ms**	**Reason**
UDP Link	10	Link between DRL and LRT (round-trip)
Space Transmission	260	Link between Ground station and ASTRA (round -trip)
GEO-Relay Link	300	Link between ASTRA and space robot in LEO (here simulated)
Total Communication Link	570	Necessary operational communication link

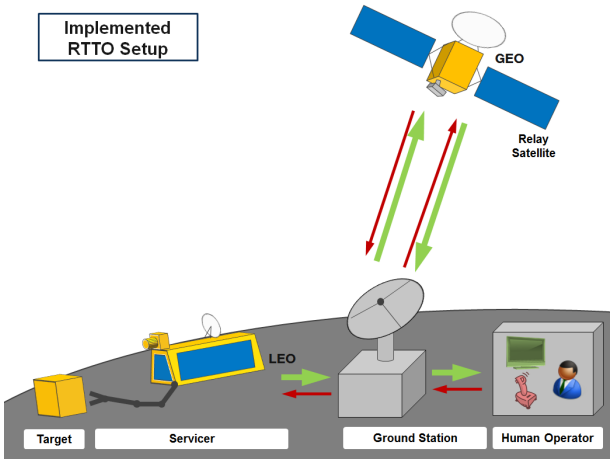

Figure 9: Real-Time Teleoperated (RTTO) Realized Measurement Setup.

Real-Time GEO Space Link

In the following, a thorough investigation of the complete end-to-end communication link is necessary. The evaluation of the communication link focused on the four main Quality of Service (QoS) parameters:

- Data rate (DR)
- Time delay (TD)
- Packet jitter (PJ)
- Bit error ratio (BER)

The QoS is evaluated by implementing the communication architecture in a hardware-in-the-loop (HIL) simulator. The LRT Real-time Attitude and On-Orbit Navigation Lab (RACOON), located in Garching (Germany), is used for this purpose [9]. It provides realistic input sensor data (e.g., optical sensors, distance measurement sensors, LIDAR) and command inputs from a human operator controlling a spacecraft. Distinct phases of such a teleoperated space debris removal mission (e.g., inspection, capture) can be executed and controlled from the mission control center (MCC) also located at the Institute. Using the sensor and command data as realistic inputs, the complete end-to-end communication chain can be implemented representing the investigated communication architecture. Even real satellite links (for example, when using geostationary relay satellites) can be included using the operational Ka band ground station, also available at our Institute. With this combined software and hardware-in-the-loop approach, a measurement of the link performance with minor deviations from the real world scenario is feasible.

Measurement Setup—The evaluation method of the four-link performance parameters is based on a hardware-in-the-loop concept that allows an almost identical hardware setup of the communication link. The complete setup was realized as an integrated simulation environment, using either representative substitute hardware, where cost prohibited the use of real space flight-hardware, or hardware which can be used in real mission operations (e.g., satellite modem, ground station, human operator workstation). The setup is depicted in Fig. 2, which shows the real scenario, and in Fig. 9, which shows the setup realized at the Institute.

Data sources, sinks and processors exist on the spacecraft (sensor data acquisition and digital data processing units (compression, packetizing, etc.)) and on ground (digital processing unit and man-machine interface). The experimental setup uses commercial terrestrial systems (COTS stereo cameras and standard PC) for the on-board systems. For the on-ground data processors, one representative setup was implemented using the Mission Control Center at the Institute. The existing network and computer infrastructure are used for data processing and to display standard telemetry. A stereo vision beamer system was implemented to visualize the captured video stream, and different control input devices were implemented for Real-Time Tele-Operated (RTTO) evaluation (keyboard, joystick, 3D-mouse and motion sensitive controller). Normally, two RF terminals would be used in the communication link for each RF-link. As the use of a real on-board modem could not be achieved due to financial limitations, the available ground station high data rate modem was used. Since the Institute has access to a 9 MHz transponder on the ASTRA W3L spacecraft for research purposes, this option was chosen to relay the data via a geostationary relay node. The complete end-to-end communication chain is shown in Fig. 10.

QoS Measurements Results—The setup described in the previous sections was used to measure the QoS of the chosen RTTO scenario. By sequentially adding the elements between the teleoperator and the human operator step by step, the influence of each element could be determined. In Table 2 the results of three performance measurement series of the video data stream are shown. The one-way time delay $t_{\downarrow,V}$, the packet jitter PJ_V, the data rate DR_V and the percentage of lost packets of the transmitted video images Lost Pack.$_V$ are presented. Measurement series #1 used a direct connection between the teleoperator and the human operator with no intermediate nodes. Measurement series #2 then added data transfer via the Modem including QPSK Modulation and Reed-Solomon Coding. The signal output at 1.2 GHz was directly fed back into the modem and the signal was demodulated and decoded. Measurement series #3 then added the real space link via a geostationary satellite. Note that the latter is in accordance with the value of 260ms given in Table 1.

Table 2: **QoS measurement results.**

Parameter	Meas.#1	Meas.#2	Meas.#3
$t_{\downarrow,V}$	[51.7]ms	[148]ms	[420]ms
PJ_V	[5.68]ms	[13.1]ms	[4.7]ms
DR_V	[3.75]Mbps	[3.77]Mbps	[3.77]Mbps
Lost Pack.$_V$	[0.024]%	[0.020]%	[0.018]%

The results of the video data stream show an increasing delay time with each additional element in the communication path. With only sensor data processing (e.g., compression) the mean delay is 51.7 ms. The complete encoding/decoding and modulation/demodulation processing increases the time delay significantly (148 ms). Adding the space link introduces the propagation delay to and from a geostationary satellite and results in 420 ms of delay. The packet jitter also increases with each additional element. For the jitter, the increase is higher for the added network transmission to and from the modem (7.42 ms). Adding the space link then reduces the packet jitter which may be correlated to internal buffering in the modem. The data rate stays constant for the measurement as the data source does not change.

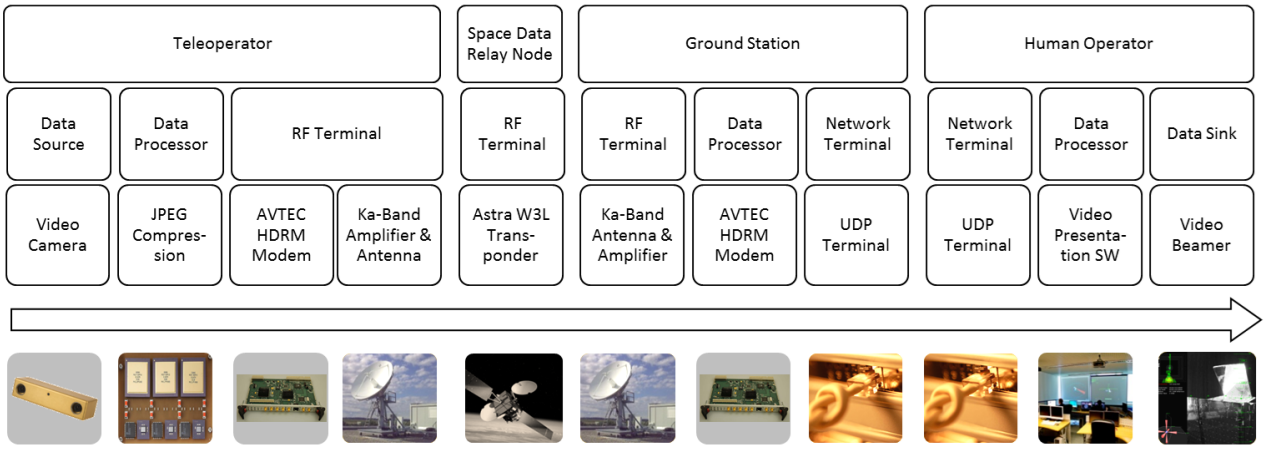

Figure 10: Example of implemented Communication Elements for Video Data Stream (Downlink).

The percentage of lost packets does not show any consistent trend but stays at values well below 0.5 %. The results and the characterization show the range of QoS values that can be achieved in a real-time communication link in space missions. Further research will correlate these measurements with the requirements from a human operator, trying to allow conclusion about the feasibility of RTTO of spacecraft.

4. Target Motion Rendering and Estimation

In this Section we first address the computer rendering of realistic camera images of a tumbling Target. These are then fed as input to a camera-based motion estimation algorithm, for validation purposes. The latter is also validated with the EPOS experimental facility of the DLR. Finally, an alternative hardware approach with a PMD-camera is presented, which is also validated with an experimental facility at the University of Wuerzburg.

Computer Rendering

The testing of the posed estimation algorithms requires images of the Target satellite as they would be captured by a real mission camera under orbital conditions. Providing an alternative to hardware-based methods to generate such images (e.g., the EPOS facility of the DLR, see below), SpaceTech GmbH developed a software tool based on the radiometric ray tracing method to synthesize these images. The two methods can be seen as complementary to each other, such that when combined, they can provide significant confidence for the verification of the image processing algorithms.

The main features of the ray tracing method are:

- Early testing of the algorithms is possible
- Full flexibility in the definition of the satellite appearance
- No configuration constraints, arbitrary state trajectory definition
- Simulation of Sun spectrum is simple, no expensive Sun simulator required
- The influence of the Earth albedo is simulated
- Distributable: every developer can have his own virtual test facility

In order to synthesize an image, the input to the software is defined by the following elements:

- Geometrical objects, positions and orientations
- Angular and linear velocities if the motion effects during exposure are of interest (motion blur, rolling shutter)
- Reflection properties of the objects
- Light sources
- Camera model

The first step is the generation of the geometrical description of the objects in the scene. This data can be imported from a CAD file which is provided by the satellite manufacturer. This model typically does not include the multi-layer insulation (MLI) which is used for thermal control of a satellite. The reflective properties of this wrinkled foil can have degrading effects on the performance of the image processing algorithms, and therefore, they have to be considered during the rendering. Modelling the MLI in a CAD Tool can take a long time to produce realistic results. A more efficient way is to 3D scan an object which is wrapped in a (structurally) MLI-like diffuse material (see Fig. 11). The scanned mesh is then fitted in software on the target part of the satellite.

(a) (b)

Figure 11: Left: mockup wrapped in paper; Right: rendering after 3D scanning and material assignment.

After the geometry is defined, the next step is the mapping the spectral bidirectional reflection distribution functions to the surfaces of the geometry. These functions which describe the scattering of light are either measured or modelled by analytical functions. In either case, the software developed is able to adapt to each function individually, otherwise, the

rendering times increase significantly due to higher noise in the image.

The scene has to contain at least one light source, which in this case is the Sun. Whereas in hardware facilities a Sun simulation can be challenging (e.g., spectrum, homogeneity, aging), in software this is a matter of assigning the correct spectrum to a parallel light source which is an acceptable approximation for the Sun. Additional artificial light sources which are on the Servicer or Target satellite can also be described by their spectrum and angular radiation profile.

The software offers the user two camera models. A simple model is based on the thin lens and requires only the focal length and aperture. If the optical design is already known, a high fidelity model can be used. Here the optics is described by the lens radii, lens thickness, indices of refraction and spectral transmission.

The detector is described by its spectral response curve which translates spectral power to a current. During the rendering process, this current is integrated over the exposure time. After pixel saturation effects are considered, the resulting pixel voltage is sampled and quantized. This value for each pixel of the detector is the final output of the software.

Fig. 12 shows a stereo rendering of a target satellite, Fig. 13 shows the same satellite from another relative position with the Earth in the background. The Earth texture was adjusted such that the average albedo value is 0.3.

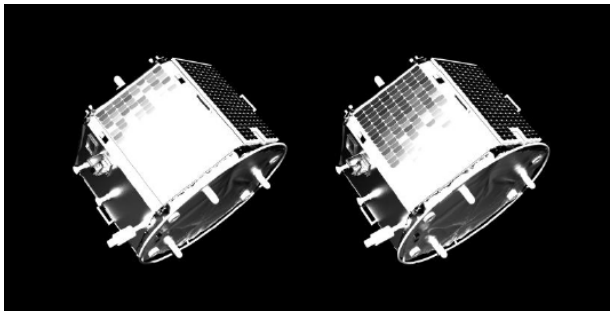

Figure 12: Rendering result of a target satellite captured in a tumbling motion. Stereo image.

The main drawback of the ray tracing approach is the long rendering time. To generate an image, several billions of rays have to be propagated through the scene. Fortunately, this is independent for every primary ray and this process can be parallelized, thus, reducing the rendering times. Therefore, the renderer was compiled into an executable and provided to DLR where the software was distributed on a computer cluster for rendering.

The ray tracing approach offers an alternative way to generate images for rendezvous missions. Environmental conditions, such as Sun and albedo, can be modelled easier than in a hardware facility and high risk trajectories (e.g., collision) can be studied without any real damage. First verification tests showed a low radiometric error ($\ll 1\%$) which could be decreased with the price of longer rendering times. Although not real-time capable yet, cluster rendering offers a good way to reduce the rendering times.

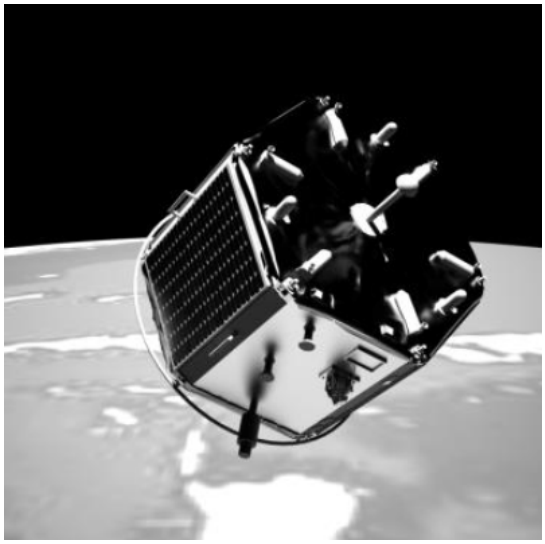

Figure 13: Target satellite with Earth in background.

Camera-based Motion Estimation

Camera-based motion estimation provides 6D rigid body motion parameters, which enables to localize and track a Target satellite in 6 degrees of freedom (DOF) for on-orbit servicing tasks. The estimated poses can be further used for motion prediction, dynamics identification, motion planning and collision avoidance (see Section 5). In general, vision-based methods can be categorized into model-free and model-based, depending on the existence of a geometric model of the object. Among model-free approachs, [10] utilizes sparse features of an image, by predicting 3D point motion with its kinematics, constrained by rigid body motion in the absence of geometric model. In contrast, in the presence of a CAD model of the Target, motion estimation is more accurate and robust to space illumination conditions, as reported in [11], [12] and [13]. When the satellite consists of point features due to junction of structures and wrinkles of MLI, point features and edges can be integrated to improve the accuracy and robustness [14].

In this paper, we exploit the geometric model of the Target to estimate its absolute orientation and position in the camera frame. Here we adopt a state-of-the-art model based tracking method based on [15], which is basically equivalent to [16], to robustly localize the moving Target during a tumbling motion. For validation, we generated and tested a large set of trajectories under various incident sunlight directions. We used real image data acquired by a robotic rendezvous simulation facility (EPOS of DLR), which consists of a Target satellite mockup, a Sun simulator with high power floodlight, and two 6 DOF robots. Moreover, photo-realistic image sequences, rendered using a computing cluster, were used to evaluate the performance of the proposed method (see Subsection above for details).

3D Pose Tracking Method—The geometric model of the Target is primarily used to predict the motion at previous known pose for robust tracking. Real-time tracking is achieved using an efficient implementation in stand-alone, single-threaded C++ code, by organizing a simplified CAD model of the satellite. In fact, for space applications we rely on standard CPUs, while we simplified the complex model provided by the original design files, in order to remove tiny surface details that are not visible at the desired range of distances,

so that we could sample visible model lines with real time efficiency.

Once we obtain a simplified model of the Target, pose tracking is achieved by projecting visible (visibility determined by depth-buffer) model features onto the image plane, and aligning them with previously detected edges on the image, by searching along the edge normal and computing the minimizer of the cost function

$$\hat{\mu} = \arg\min_{\mu} \sum_{i}^{n_p} ||\mathbf{s_i} - \mathbf{y_i}(\mu)||^{\mathbf{2}} \quad (1)$$

where projection of 3D sample points onto a camera, $\mathbf{y}$ at pose parameters μ, and $\mathbf{s}$ are 2D image coordinates of the nearest edge corresponding to the projected 2D points of the model coordinate, and n_p is the number of valid sample points respectively. The Jacobians can be easily computed from the re-projection error, and the pose parameters μ are determined using Gauss-Newton optimization, iteratively refining the pose estimate until it converges.

Although image saturation, shadows, specularities and feature occlusions pose well-known difficulties, the implemented method has been shown to be robust and accurate enough during the approach to the tumbling satellite. This is achieved by introducing adaptive search length along the normal, proportional to the ratio of the object size and distance to the camera. In some cases, where the image is highly saturated, morphological pre-processing such as top-hat filtering is employed. This filtering preserves edges of the image, while removing ambiguous edges because of specularity.

Experiments—The visual tracking method is validated using ground truth data, generated through both software (rendering) and hardware (real camera images) simulation systems. Both methods were able, albeit to a different extent, to provide realistic camera optics, motion of the Target, Sun illumination and optical characteristics of the Target surface. On one hand, the software simulation relies on physical models, and is suitable for generating a trajectory with accurately known ground truth, despite the difficulty of simulating actual surface properties. On the other hand, hardware simulation using real camera images is more practical, despite some ground-truth inaccuracies due to random and systematic errors of robot-based measurements and camera calibration, and less realistic sunlight and background illumination conditions.

For the photo-realistic rendering, the rendering software was used to produce realistic images through the ray tracing method. These include stereo cameras with a baseline of 40cm, a simple Servicer satellite model, and a complex, photo-realistic Target model. The program simulates camera optics, material properties of the Target and sunlight spectrum. Both satellites are at 400 km altitude, and the Earth is modelled as a sphere with constant albedo of 0.3. Since ray tracing is computationally intensive, we employed cloud computing parallelism using the DLR computing cluster, to implement a given trajectory in a relatively short time. Note that on a 2.2 GHz computer, for a 1024x1024 image size and 1600 samples/pixel, the rendering time was about 3 minutes.

For the real camera image sequence, several ground-truth trajectories, consisting of in-plane and out-of plane motion, were tested using the EPOS facility and real camera images with resolution 640x480. The EPOS facility reproduces a complete satellite rendezvous system, space environment and optical characteristics, by using:

- mockups of Servicer and Target satellites
- motion trajectory using 6 DOF robots
- high power floodlight with the Sunlight spectrum
- multilayer insulation (MLI) on the satellite surface

More information on the facility can be found in [17].

Visual tracking has been extensively tested on various trajectories, to assess the performance of the method quantitatively (referred to ground truth) and qualitatively (visually superimposing matching edges), using both photo-realistic and real image sequences. The accuracy and robustness of the employed method under illumination variation, specularity and difficult motion have been verified. An overall accuracy of 1 degree in rotation and 1% in translation is achieved in the range 7m to 2.5m, where the satellite edge features are dominant over the background clutters. The tracking accuracy in general increases as the Servicer is closer to the Target, provided that sufficient features remain visible in the camera field of view. The accuracy in rotation and translation of each tested trajectory, based on both real camera images and rendered images, depends strongly on illumination. Tracking results from photo-realistic rendering, shown in Fig. 14 c and d, indicate similar error distributions with respect to the real image, Fig. 14 a and b. However the average error is significantly lower, because of illumination difference and less background clutter as it can be observed in Fig. 15. Note that, the Targets used for rendering and images from EPOS facility as well as illumination conditions are different. Hence the comparison of the two validation methods, based solely on common a trajectory, may not be relevant here.

At relatively large distance, pure edge-based tracking fails due to ambiguity of background clutter and specularity. The standard tracking method is improved by introducing adaptive search length along the edge normal and non-linear edge preserving filter such as morphological processing. This can be clearly observed in Fig. 16 c and d, where projected edges correctly overlaid on the detected image. We observe that in a few cases, an abrupt jump in pose estimation appears (14 a), because of convergence of Gauss-Newton optimization at local minima, which can be improved by imposing a motion model in the Kalman filter framework in future work.

Summary—We have performed an extensive testing for real-time estimation of 6 DOF motion of a Target satellite under harsh space lighting conditions based on real camera images and photo-realistic rendering. The performance of vision-based 3D tracking in the critical close range, with challenging illumination conditions and motions, has been analyzed. In general the accuracy depends on illumination, the pose and visible Target features. The photo-realistic rendering can be considered as an alternative method for validation and verification of motion estimation algorithms under space lighting conditions, although the modelled MLI is not precisely representative of actual MLI.

PMD Camera-based Motion Estimation

The use of a stereo vision system, as described in the previous Subsection, is one of the popular imaging technique, also for space applications. Owing to several years of worldwide research in stereo vision based imaging, the technology enjoys a great deal of support. On the other hand it has its limitations, susceptibility to lighting conditions, correspondence problem among others.

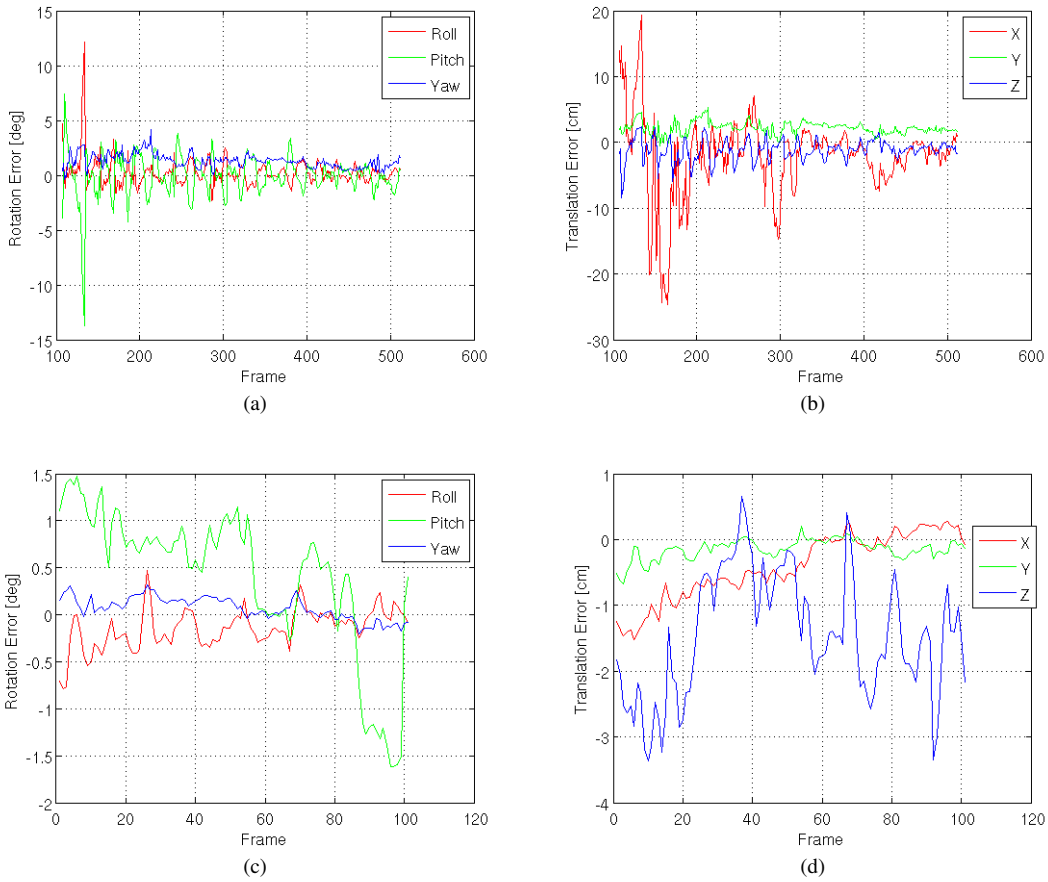

Figure 14: 3D tracking on real image from a full-scale mock-up (a & b) and photo-realistic images from a Model (c & d). Note that, the first 200 frames are badly illuminated, however morphological pre-processing with adaptive search length along edge normal improved the result.

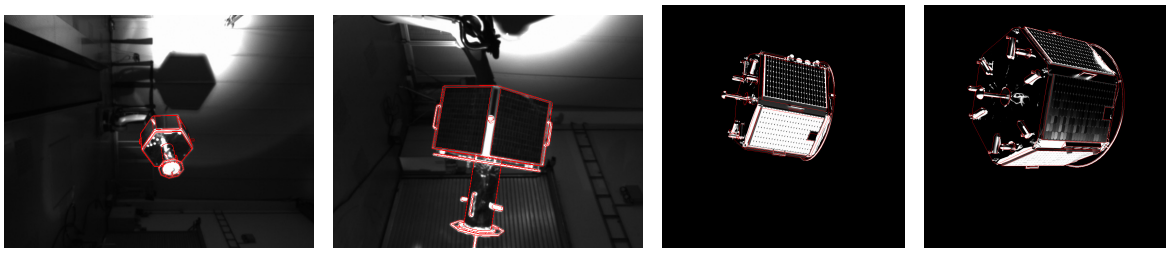

Figure 15: Some frames from the tracking sequence: real camera image from a full-scale mock-up, frame 39 (a) and frame 425 (b), and photo-realistic rendered images from the Model, frame 3 (c) and frame 101 (d).

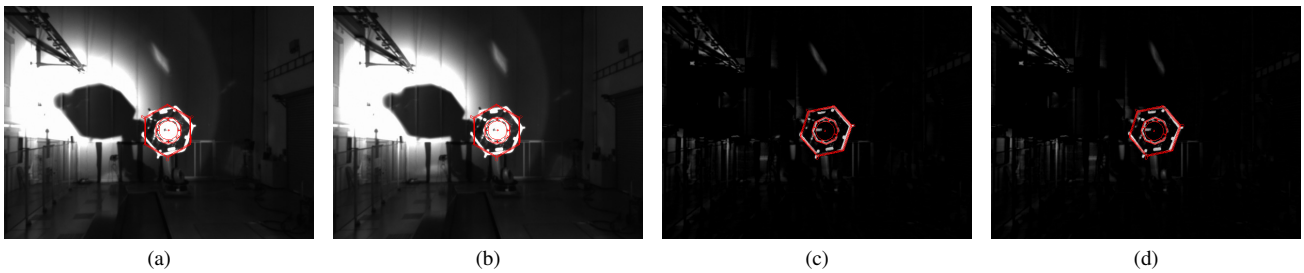

Figure 16: Edge-based tracking fails, with various background clutter (a & b), while adaptive correspondence search length along the normal and morphological preprocessing succeeds(c & d)

In a new approach, a state-of-the-art ToF (Time of Flight) based 3D imaging sensor, PMD (Photonic Mixer Device), has been tried for space applications to tackle the problems earlier negotiated by stereo vision camera, to evaluate its strengths, limitations, complementarity with respect to stereo vision camera, adaptability of exiting image processing techniques for relative motion and pose estimation of a spacecraft and to detect and predict collisions by combining range measurements of PMD with estimated relative navigation information.

In the following, basic principles for the PMD camera are briefly presented, as well as a relative navigation algorithm. Enhancements to the PMD camera are discussed in the following Subsection. Results for collision detection and avoidance techniques based on PMD measurements are presented in Section 5.

Navigation Sensor— Our chosen imaging sensor for close range relative navigation has been Photonic Mixer Device (PMD) sensor based 3D range camera PMD[Vision] CamCube 2.0 (17). PMD sensors are 3D imaging sensors developed by PMDTechnologies GmbH.

Figure 17: PMD[vision]® CamCube 2.0 with one IR illumination unit on either side of the imager.

The camera uses a modulated Infra Red (IR) light to illuminate the scene. The light reflected from the Target is then demodulated and compared with a reference electrical signal using auto-correlation technique to determine the phase shift between the two signals. The corresponding range is then inferred from the phase shift. The auto-correlation process is performed at hardware level in each pixel, drastically reducing the post-processing computational requirement. For more about the working principle interested readers are referred to one of the many literature references [18] about the PMD sensor. The work carried out University of Würzburg is based on PMD[vision]® CamCube 2.0. This camera can work with modulation frequencies ranging from 19 MHz to 21 MHz and with frame rates up to 25 frames per second and offers a maximum lateral resolution of 204 x 204. Such a high frame rate makes the sensor an ideal visual navigation aid, particularly when motion estimations are to be made in real-time and to support semi-autonomous operations via tele-operations involving human operators on ground. Although the maximum measurable unambiguous range of camera is 7.5 m, it has been shown by a peer researcher of University of Würzburg that by using multiple modulation frequencies, the measuring range can be extended theoretically up to 75 m and experimentally has been proven up to 22 m [19].

Algorithm—The pose estimation algorithm is based on the information provided by the PMD camera. Throughout the process of identifying the object and estimating its relative position and attitude, the amplitude (a measure of Signal to Noise Ratio (SNR) of optical signal) and depth information

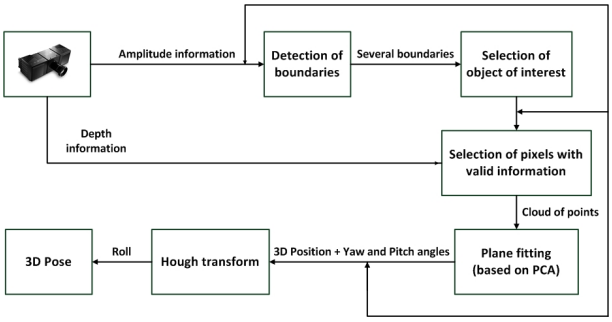

Figure 18: Block diagram depicting stages of the pose estimation algorithm.

are used. Within this algorithm, the overall process of estimating the pose is subdivided into different stages. These stages are depicted in Fig.18. In the diagram the usage of the two fore-mentioned types of information provided by the camera can be observed. The estimation of 6 DoF is performed in separated steps for the roll angle and the rest of the parameters. By making use of plane fitting for the estimation of the position and the yaw and pitch angles, an assumption about the geometry of the object is made, that is, that the object is formed by planar surfaces. Additionally, in order to be able to make use of the Hough transform, the algorithm assumes in parallel that straight edges are available around the object.

Experiments and Results—For the experiments, a mock-up model built in University of Würzburg was used. The model consists of a 30 cm side cube and two rectangular appendices of 25 cm $\times$ 50 cm representing the solar panels are attached to opposite sides. Both the model and the camera were attached to two KUKA manipulators in order to simulate a variety of precise relative motions. For all the experiments, the camera was held statically, while the model was moved along a predefined trajectory. The new test facility (see Fig. 19) developed in FORROST to simulate Rendez-Vous and Docking scenarios was used to test the algorithm. The developments made in setting up the on-ground test facility to provide space-like test conditions and its performance characterization for selective close range scenarios are discussed in [20].

For the developed pose estimation algorithm, position estimation in 3D with a relative error of less than 1 % and

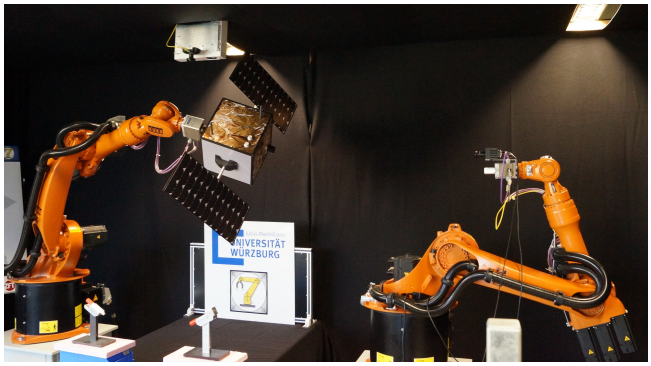

Figure 19: Hardware-in-the-loop testing facility at University of Würzburg equipped with satellite mock-up model (left) and PMD camera (right).

Table 3: **Results of the velocity estimation for the different experiments.**

Motion	Reference	Estimation	Relative Error
Translation X	5.13 cm/s	5.24 cm/s	2.1 %
Translation Y	5.84 cm/s	4.58 cm/s	5.3 %
Translation Z	5.02 cm/s	5.02 cm/s	0.4 %
Rotation Yaw	5.5 °/s	5.01 °/s	8.8 %
Rotation Pitch	6.5 °/s	6.07 °/s	6.6 %
Rotation Roll	5.6 °/s	5.73 °/s	2.3 %

velocities estimation with errors ranging from less than 1 % and up to 8.8 % were achieved. The algorithm has been tested with simple motions. Table 3 enumerates features and results of experiments for rotational and translational velocities characterization. The progressive developments and results achieved during the course of the project are made available in detail through several publications [21], [22] and [23].

Sensor Enhancement

It is the first time that a PMD imaging sensor was proposed for such a space application scenario. As with any sensor, this sensor too calls for substantial evaluation of its performance under space conditions, typical to those found in LEO for On-Orbit Servicing mission such as DEOS mission. Our research efforts towards this specific topic has made a promising start by tackling one of the most commonly faced problems, dealing with the specular reflections, a problem faced not only by imaging sensors with active illumination but also with conventional imagers used in space such as monocular and stereo vision systems.

Multi-Perspective Imaging—A new technique, termed MPI (Multi Perspective Imaging), in which illumination units of a PMD camera are spatially arranged to illuminate and image a scene from different perspectives and to blend the data to produce more reliable data of the scene has been developed. This has emerged with promising results in addressing one of the hurdles to be cleared towards space preparedness of a PMD camera. Figure 20 depicts this technique of building highly refined image by fusing data from several frames.

The above process identifies bad pixels susceptible for specular reflection and replaces them with reliable and consistent data from other measurements. As the measurements captured by the camera are eventually provided to a motion estimation algorithm, whenever there is loss or quality degradation of data due to specular reflection, then it affects the estimation made by the motion and pose estimator. This might even result in temporary loss of estimation until the satellite surface is clearly visible again. Hence the developments reported here are significant in ensuring quality of measurement and its continuity and thus accurate functioning of subsequent subsystems of motion estimation and autonomous collision detection and avoidance.

Experiments and Results—Figure 21 shows the corresponding experimental setup done in proximity operations test center to test functioning and evaluation of the MPI technique. The setup uses two KUKA industrial robots and a Polaris R Spectra IR optical measurement and tracking system. They are used for precise positioning of the IR emitter and the imager respectively. Two test objects were used for the experiment.

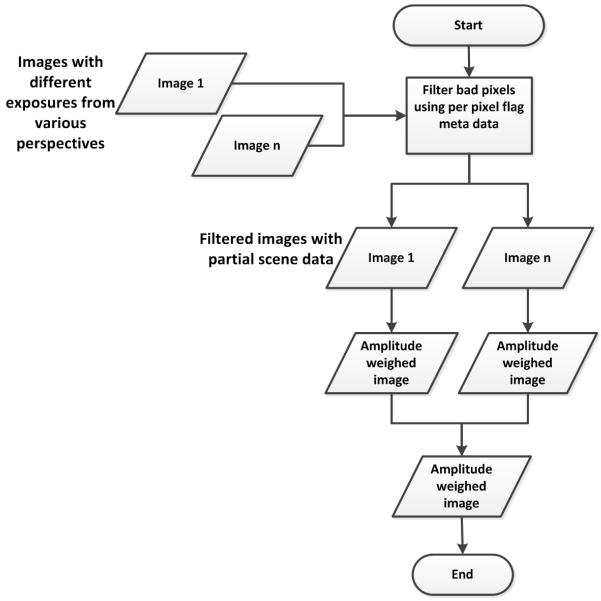

Figure 20: Images with multiple exposure time taken in a single perspective are combined by filtering and amplitude-weighing to produce one image per perspective.

One was a MLI like material, highly reflective and has uneven surface because of wrinkles. The other object had a diffusive surface. Both surfaces were placed at 1.8 m from the sensor plane of the imager. The test planar surfaces are not kept parallel to imaging plane. We expect an overall variation of the test surface between 1.8 m to 1.9 m with respect to the sensor plane.

After capturing images from 7 different perspectives, images were chosen such that the one image from each of these perspectives provides information in various image regions, compensating for the erroneous data present in the other images. The measurements corresponding to the highly reflective surface shows significant improvements. This region has a depth value in the range of 1.8 m$\pm$0.1 m. This is in good agreement with the reference distance which is about 1.8 m.

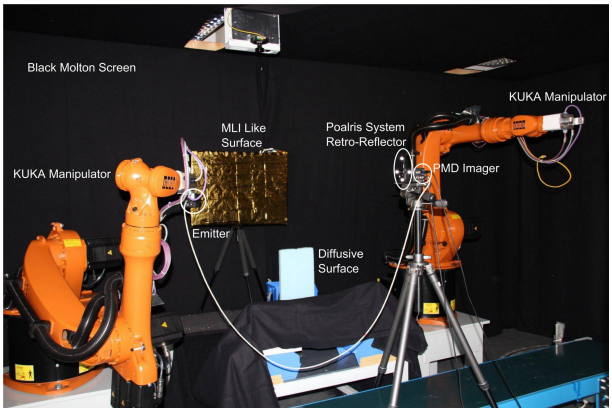

Figure 21: Test scene with MLI like surface and a diffuse surface surrounded by black screen for contrasting and non-reflecting surrounding conditions. Placement of IR emitter is controlled through KUKA robot. The PMD imager is localized using Polaris system.

Through these experiments we have demonstrated that the concept to image a scene from several illumination perspectives and to combine the reliable measurements from these perspectives into a single image is realizable. The technique, however, is not autonomous in deciding the exposure time and which positions are best suited to illuminate the scene. So far these issues are dealt with by inspection of the measurements and of a conducive set of data chosen for final processing. Nevertheless, the validity of the concept and proof of its effectiveness are intact. These developments along with relevant details of the technique and experimental data are detailed in [24].

5. CONTROL METHODS FOR AUTONOMY

In this Section we address two different functionalities for robotic and spacecraft autonomy. At first, we describe a new method for planning feasible robot trajectories for grasping a tumbling Target satellite, for the scenario described in Section 2. We then address the autonomy for the relative motion between the Servicer and the Target, to include collision detection and avoidance.

Semi-autonomous Grasping

As already described in Section 2, the semi-autonomous operational mode is based on the generation of a feasible trajectory of the robot manipulator, by means of a motion planner. The semi-autonomy refers here to the fact that the operator defines the grasping point on the Target, either thanks to prior knowledge of its geometry or by inspection. However, the tumbling state of the Target (orientation and angular velocity), and its propagation in time, is generally unknown. Furthermore, the communication link coverage is limited within a given orbit, due to possible Earth occlusion or lack of a direct link, in the cases of a link with a geostationary satellite or of a direct link to ground respectively.

These facts pose some challenges with respect to being able to satisfy all motion constraints for a given tumbling state of the Target in a given operational window. This point is made evident in Fig. 22, where the trajectory of a preselected grasping point on the Target is shown for an arbitrary initial orientation and angular velocity of the Target. Due to the nonlinearity of this motion, a limited link coverage means that possible grasping times will require having to reach the grasping point in different positions and orientations relative to the robot. The feasibility of this maneuver will be affected by the Target geometry (e.g. possible collisions with solar panels) as well as by the robot motion constraints (workspace limits, kinematic and dynamic singularities [1], internal forces during stabilization).

For this reason, we developed a grasping control method which is able to provide a feasible trajectory for any tumbling state of interest. We first parameterize these tumbling states through a set of parameters $\mathbf{p}_{task} \in \Re^{N_p}$, where N_p is the dimension of the task parameter space. For the most general case, $N_p = 6$, for arbitrary orientation and angular velocity (note that the relative position can be kept constant by the Servicer orbital control system). The motion planner is then used to generate solutions off-line for a given predefined region in $\mathbf{p}_{task}$, at preselected grid points (an on-line implementation of the motion planner is not possible due to the computational effort it involves, as described below). These solutions are stored in a lookup table for later use on-line. In the on-line setting, we implement a Target motion prediction algorithm, with which we can determine, at a given time, or

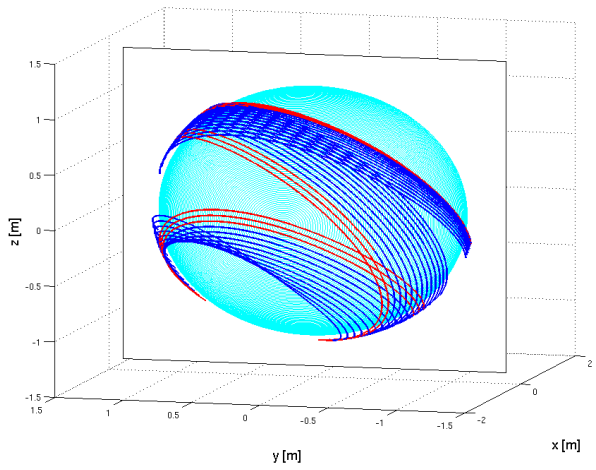

Figure 22: Trajectory of grasping point shown in Fig. 1 for an initial angular velocity [-2 -4 -2] deg/sec and communication link coverage for half-orbit period (blue line) and 8 minutes (red line). Centre of mass of Target is in coordinate frame origin.

for a given operational window, in which subregion of $\mathbf{p}_{task}$ the Target is. Given this information, we extract from the motion planner lookup table a feasible reference trajectory with which we can safely accomplish the grasping task.

In the following, details on the motion prediction and on the motion planning are provided. More details on these methods can be found in [25] [26] [27]. The motion tracking task which runs on-board is not addressed here. However, as mentioned before, the on-board controller takes account of modelling and motion prediction errors, with help of the on-board sensors (e.g. a stereo camera on the robot end-effector). It is assumed that these disturbances are small and that the reference trajectory can still be considered valid in its vicinity. In order to help make this assumption valid, the identification of the model parameters is possible, as discussed in the next Section. Furthermore, it is useful to note that this control approach, which is based on tracking a reference trajectory, provides a guarantee of high-performance and safety of the robot maneuvers, in comparison to a classical regulation control, due to the highly nonlinear and constrained nature of the given problem. An overview of these functionalities is given in Fig. 23.

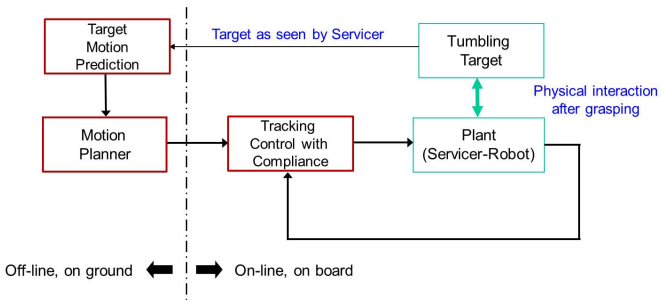

Figure 23: Block diagram of the semi-autonomous operational mode for the grasping task.

Target Motion Prediction—The Target motion prediction task consists in providing knowledge of the Target pose (position and attitude) in the future time. This is in support of the motion planner or even of the operator: for the first, the motion prediction needs to cover the computation time of the planner, which is typically in the order of 30 seconds, as well as the synchronization and duration of the approach phase of the robot grasping maneuver; for the second, the motion of the chosen grasping point on the Target may be non-intuitive (for a general tumbling motion, as described in Fig. 22) and as such may be difficult for the operator to predict.

First developments of a motion prediction functionality were already presented in [25], where the prediction method based on nonlinear optimization is also described. Other approaches exist in the literature (e.g. [28] [29] and the references therein), which however are based on an on-line approach (Kalman filter) for shorter prediction times. The salient operational features of the method in [25] are presented here for clarity. The method involves two steps:

- Observation phase: the Target pose is measured for a period of 100 seconds by means of a visual sensor on board of the Servicer (e.g. visual camera, LIDAR). From these measurements, motion estimates are computed (see Section 4).
- Prediction phase: the motion estimates of the Observation phase are extrapolated in time for another 100 seconds. This is done by identifying a suitable dynamic model of the Target and integrating its equations of motion with partly measured and partly identified initial conditions.

The application of this method on the pose estimates derived from experimental and simulated data described in Section 4 is planned as future work and will be published separately. However an example of a simulated trajectory can be found in [25] . Note that the noise in the pose estimates plays a fundamental role in the accuracy of the motion prediction. Statistical evaluations can be carried out to determine an acceptable level of the noise (e.g. standard deviation) for the task at hand. This then sets a performance requirement on the visual sensors used on-board, and on operational conditions, such as the observation distance and duration. Recently, statistical evaluations were performed for a simulated LIDAR sensor at a distance of 1,5 meters from the Target and for an observation time of 100 seconds, with satisfactory results in the motion prediction errors (grasping point position error under 12 cm after 100 seconds prediction time).

Motion Planning— The motion planner solves a nonlinear optimization problem with nonlinear constraints. The nonlinearity stems from the nature of the kinematics and dynamics of the robot manipulator, which is enhanced by the fact that the latter is mounted on a free-floating base. The motion constraints consist of the typical robot joint box constraints (position, velocity, robot internal torques during the stabilization), as well as (self-)collision avoidance, robot singularities (kinematic and dynamic) and operational constraints (e.g., desired homing-in angle to support the visual servo, other).

To solve this type of motion planning problem requires extensive computational time [27]. This is principally due to the fact that the robot has a free-floating dynamics, which requires numerical integration of its equations of motion, for any given motion of the manipulator. Also given the iterative nature of numerical nonlinear solvers, the result is a computation time in the order of 30 seconds. Furthermore, due to the nonlinear nature of the problem, an appropriate initial guess needs to be provided in order for the motion planner to converge to a good feasible solution, if to one at all.

It is for this reason that the off-line approach described above was developed, after which (near to) globally optimal solutions are computed, by means of global search strategies, for a whole range of possible Target tumbling states. In [27], the task parameter space was defined to have four entries: three for the orientation of the Target rotational axis (assumed inertially fixed), and one for the angular rate around it. When discretizing the task space into grid points, for each one of the orientation parameter grid points results a position of the predefined grasping point on the Target in inertial space (omitting orbital dynamics), as shown in Fig. 24. For each one of these points, a subset of points which discretize the angular velocity of the Target are defined, for which a feasible grasping solution is generated with the motion planner (if one is found). Finally, projecting the Target motion prediction onto this grid, as shown in Fig. 24, simply requires finding the grid point which is closest to the given trajectory, to select the closest feasible trajectory from the lookup table. Clearly, if no solution is found within the 100 seconds prediction time, the whole loop is repeated.

Autonomy, Collision Detection and Avoidance

In this section an autonomous collision detection and avoidance system for Rendez-Vous and Docking (RvD) and OOS maneuvers is presented. It was developed alongside of the previously mentioned PMD-based motion estimation (see Section 4) but is not restricted to it. It predicts relative trajectories of the involved spacecraft and checks for possible collisions. In case of a predicted collision, an avoidance trajectory for the Servicer spacecraft is calculated and the required ΔV is provided.

Autonomous Collision Detection—In the frame of the FOR-ROST project a collision detection system was developed at University of Würzburg that is especially designed for

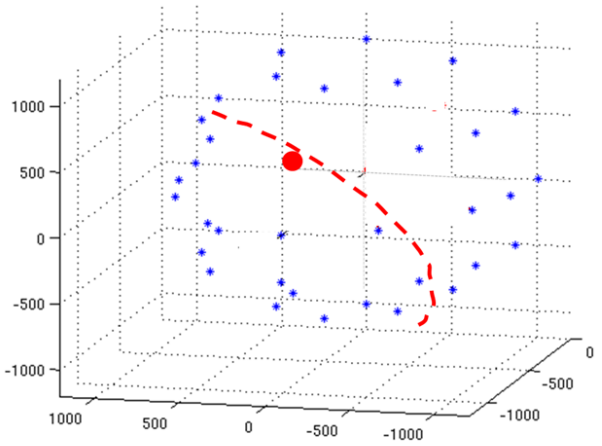

Figure 24: The set of grid points (in blue) represent the region of interest for the orientation of the Target (a hemisphere). The origin of the coordinate frame is in Target centre of mass. The blue grid points represent the positions of the grasping point for each orientation. The red line represents a given motion prediction of the grasping point and the red dot the chosen solution in the grid.

OOS and RvD maneuvers to passive objects in space. The system is based on pose estimation from the 3D imaging sensor, PMD camera, and utilizes the relative pose and range estimates of the observed Target to predict its relative position trajectory. Trajectory prediction is performed on-line using the Hill-Clohessy-Wiltshire equations [30] for circular orbits or with the Tschauner-Hempel equations [31] for elliptical orbits and predictions are updated with each new set of pose estimates. Simulations have shown that the Hill-Clohessy-Wiltshire equations already cause significant deviations for slightly elliptical orbits with eccentricities above 0.1. This requires the usage of a suitable solution for non-circular orbits, thus the Tschauner-Hempel equations together with their solution by Yamanaka and Ankersen [32] were implemented.

Potential collisions along the predicted trajectory are detected in a sliding time window of up to 10 minutes with the help of geometrical intersection tests on 3D models of Target and Servicer spacecraft (more precisely intersection tests on multiple oriented bounding boxes surrounding the actual two spacecraft). Thus the spacecraft geometry is also taken into account. The system is flexible to be used with arbitrary spacecraft geometries and relative trajectories on circular as well as elliptical orbits around Earth. It is designed to raise alarm for possible collisions and to provide spatial and temporal characterization of foreseen collisions. The complete work flow of the algorithm is depicted in Fig. 25.

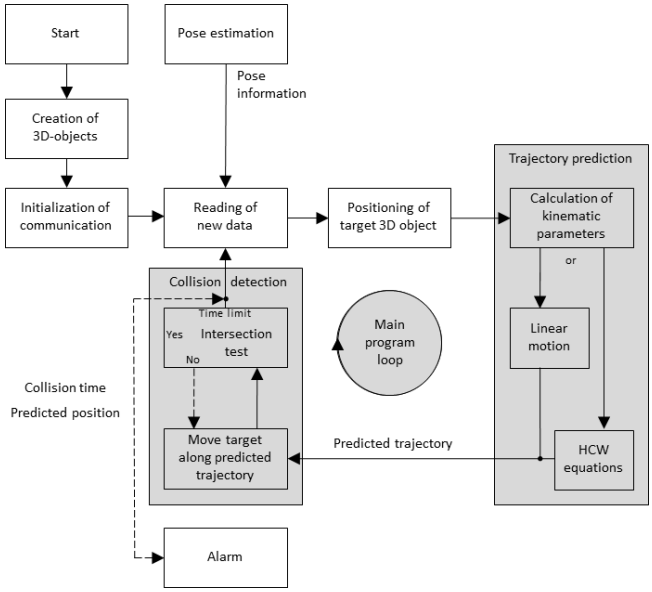

Figure 25: Work flow of the collision detection algorithm illustrated as block diagram.

Different scenarios including approaching, departing, rotating and by-passing were conducted in the test hardware-in-the-loop test facility at University of Würzburg (see Fig. 19 in Section 4). With the help of these scenarios the functionality of the developed algorithm in common RvD and OOS maneuvers was evaluated and confirmed. These results along with detailed description of the algorithm are reported in [33].

Real-time Behavior and Synchronization—Special focus was set on investigation of the real time behavior of the developed systems. For this purpose the hardware-in-the-loop test facility could be used and extended. Thus several test scenarios were designed and performed to prove the stability and real-time reliability of the developed systems. Especially measurements on in-system delays were performed to determine the different timing delays of the sub-systems. Further information on the testing facility and its characterization are published in [20].

Autonomous Collision Avoidance— To augment the previously described collision detection system, collision avoidance was also treated in this project, making it a complete system. Based on the output of the detection system – the predicted time of the foreseen collision as well as the positions of the spacecraft at that time – an escape trajectory for the Servicer spacecraft together with the required ΔV for the maneuver is computed.

The collision avoidance algorithm calculates an adequate maneuver designed to avoid a foreseen collision and brings the Servicer to a safe hold point from where a new approach maneuver can be commenced or where the spacecraft can stay safely until commanded further by the ground operators, depending on the operation strategy. The system relies only on the previously explained pose estimation (see Section 4) and collision detection (see above) algorithms, and is independent from other spacecraft subsystems besides the visual sensor it is using. Computed maneuvers are as simple as possible (only one single thrust/ΔV) to avoid possible complications with other subsystems that might be necessary to execute complex maneuvers, while still being able to react to any hazardous situation and trajectory. Avoidance trajectory computation is not restricted to any specific type of approach trajectory, but applicable to any arbitrary relative trajectory. There is a set of conditions leading to the initiation of a collision avoidance maneuver. A velocity profile (as an arbitrary function such as linear or step-wise) can be applied together with an approach corridor (cone shaped) and a minimum distance threshold. In addition, to trigger a collision avoidance maneuver the system requires either a detected collision or a system command or an user input. ΔV calculation for a collision avoidance maneuver takes pre- or user-defined targeted hold point on V-bar into account in order to create optimal conditions for a second approach. So depending on mission and situation conditions a target hold point can be chosen. Hold points on V-bar are force-free with almost no relative drift with respect to the Target and thus minimize the fuel consumption. In Figure 26 a possible collision avoidance trajectory for a given arbitrary Servicer approach trajectory is shown.

Computed escape trajectories are checked for possible further collisions on the escape trajectory itself to provide long-term safety after an avoidance maneuver. The functionality of the whole system was demonstrated with the help of appli-

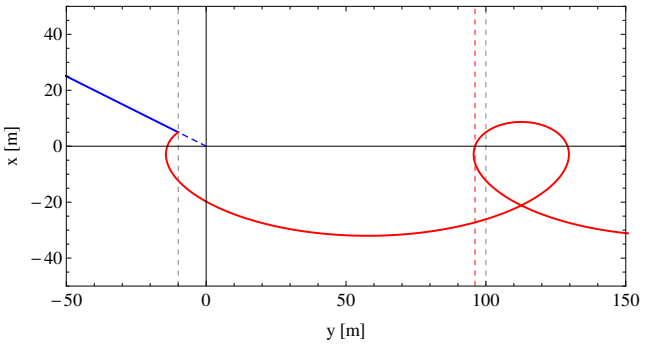

Figure 26: Servicer approach trajectory (blue) from arbitrary direction and according collision avoidance trajectory (red).

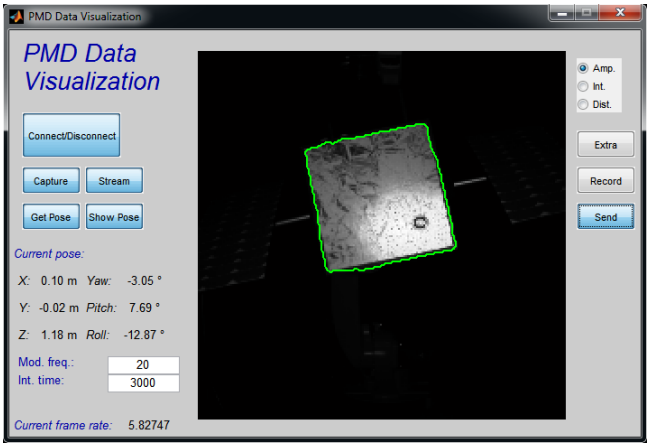

Figure 27: Pose estimation software including video live stream of the target satellite with overlaid detected borders as well as estimated relative position and orientation of the observed target.

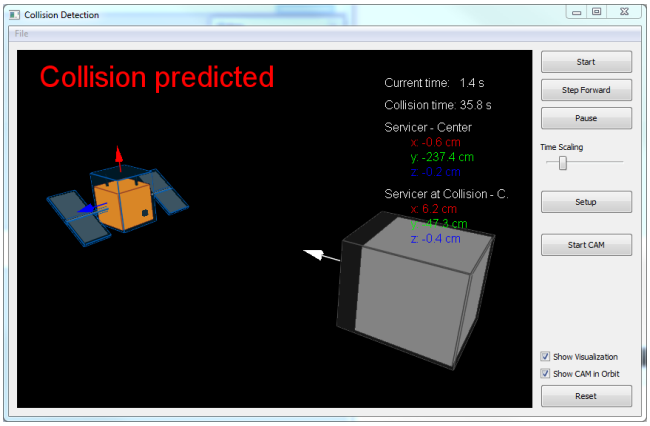

Figure 28: Collision detection and avoidance software showing a 3D visualization of the scene and the detected collision parameters.

cation examples running in the hardware-in-the-loop testing environment described in the previous sections. Further information on the described algorithm as well as the tests performed was published in [34].

Collision Avoidance Assistance System—During the development of the previously described pose estimation algorithm (see Section 4) and collision avoidance algorithm, focus was also set on processing and visualizing sensor information in such a way that a tele-operator can easily understand the provided information and is aware of the real relative position and orientation of the Target spacecraft to be able to make the right decisions.

Figure 27 shows the pose estimation software, whereas in Fig. 28 the collision detection and avoidance software in operation is shown. The pose estimation software displays a live video stream of the PMD camera view overlaid with detected borders of the target spacecraft and the estimated relative position and orientation computed by the algorithm. Thus the tele-operator can easily grasp the conditions in a scenario. This is supported by the collision detection and avoidance software which provides a freely rotatable and movable 3D visualization of the Target and the observer spacecraft including safety bounding boxes as well as velocity vectors. In the case of a foreseen collision, it additionally provides the predicted time and position of the collision and allows the user to execute a collision avoidance maneuver. Different levels of autonomy are possible in this design. The system can act as an information provider and adviser while leaving the actual decision and command to the tele-operator, but it can also act autonomously by executing an evasive collision avoidance maneuver, if it is reasonable (based on the conditions described in the previous section). As already mentioned in the corresponding sections both systems were extensively tested in the hardware-in-the-loop testing facility of University of Würzburg. For further reading the reader is referred to [34].

6. System Parameter Identification

We present here research work in the field of parameter identification, specifically for a free-floating robot in orbit. This includes the identification of any relevant system dynamics, to include flexible appendages and fuel sloshing.

To improve path planning and tracking capabilities as well as efficiency in energy consumption by reducing the control effort, the dynamic model must be known to a sufficient accuracy. Normally, the manipulator properties stay constant in space, but due to fuel consumption the parameters of the satellite base will change significantly. Furthermore, after grasping an unknown target object the complete dynamic behavior of the new system will change dramatically. For these reasons, an identification method is indispensable to obtain the inertial parameters like mass, center of mass and moments of inertia of all system components, especially the satellite base (Servicer) and the unknown Target. The workpackage in the FORROST project for parameter identification was spit into three main parts: finding proper excitation trajectories, the analysis of different identification methods for rigid body models and in addition the influence of flexible appendages and sloshing effects to the free-floating robot dynamics and their parameter identification.

Trajectory Optimization

In the first part we addressed the problem of finding exciting trajectories. This can be formulated as a constraint nonlinear optimization problem. The new approach in the presented method is the parameterization of the trajectories with optimized B-splines. Experiments were carried out on a 7 joint Light-Weight robot with torque sensing in each joint. Thus, not modeled joint friction and noisy motor current measurements must not be taken into account. The estimated dynamic model was verified on a different validation trajectory. The results show a clear improvement of the estimated dynamic model compared to a CAD model. More details on the described methods can be found in [35].

Analysis of different Identification Methods for Rigid Bodies

As a second step in the project, we analyzed different identification methods for a free-floating system, to identify the most efficient. The details of this work can be found in [36]. We used two torque sensing methods, referred to here as Modified Recursive Newton-Euler Algorithm (MRNEA) and the Reduced Dynamics Algorithm (RDA). Additionally, identification methods based on the conservation of momentum (CM) and conservation of energy (CE) were analyzed. The advantage of the RDA algorithm is the fact that no translational velocity measurements of the satellite base are

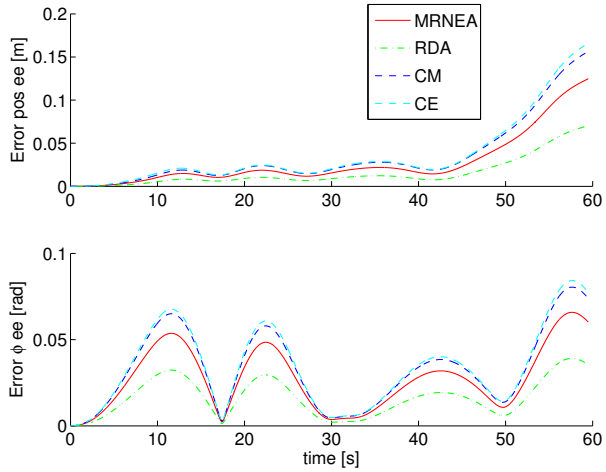

Figure 29: Time history of the error of end effector position and orientation.

needed. The results of a simulation study are shown in Fig. 29. It turns out, that the RDA methods seems to be the most convenient solution.

Additionally to this analysis, we simulated the influence of orbital disturbances to the identification process and came to the conclusion, that the these have measurable effects to the identification process and should be taken into account.

Analysis and Identification of Flexible Appendages and Sloshing Effects

Next, we focus on two disturbing dynamic effects, which the free-floating robot control has to cope with during a realistic OOS mission: flexible appendages and liquid fuel sloshing. All details on this work can be found in [37]. In Fig. 30 the principle parts of the addressed OOS system are sketched. The manipulator is assumed to have both rigid joints and links.

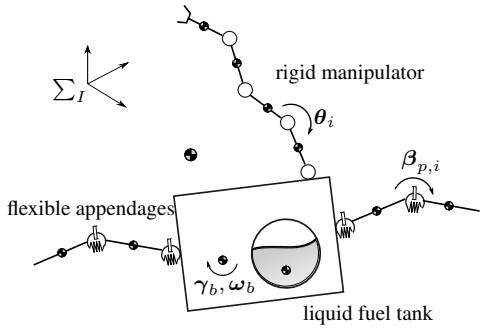

Figure 30: Principle free-floating robot with flexible appendages and liquid fuel tank with manipulator joint position θ_i, flexible joint position $\beta_{p,i}$, γ_b and ω_b as orientation and angular velocity of the base satellite respectively.

Flexible Appendages— For modelling flexible appendages like solar panels we assume rigid panel plates and flexible rotational joints connecting them. The general equation of motion for a free-flying robot without any external forces and moments (free-floating), is extended with solar panels connected with rotational joints. The robotic manipulator itself is assumed to have no flexible joints. For a free floating system the equation of motion can be expressed as

$$\hat{\boldsymbol{H}}\ddot{\boldsymbol{y}} + \hat{\mathbf{C}} + \mathbf{K}\delta\boldsymbol{y} + \mathbf{D}\dot{\boldsymbol{y}} = \boldsymbol{\tau} \tag{2}$$

where $\hat{\boldsymbol{H}}$ is the generalized inertia matrix, $\mathbf{y}$ contains the manipulator joint positions as well as the joint positions of the flexible appendages and $\hat{\mathbf{C}}$ is the generalized nonlinear velocity dependent term. The robotic joint torques are represented by $\boldsymbol{\tau}$, see [36]. The diagonal matrix $\boldsymbol{K}$ contains the stiffness parameters k_i of each flexible panel joint and the diagonal matrix $\boldsymbol{D}$ contains the velocity depending viscous damping parameters d_i.

For the identification of the flexible modes of the appendages we use appropriate manipulator excitation maneuvers. There are designed such that they contain excitation frequencies which suit the given identification task. We assume an *a priori* knowledge of the orientation of appendages rotational joint axes. However, for reasons of simplification, we assume that all these joints are parallel. To obtain the highest response in the appendages to the robot excitation maneuvers, we aim at inducing a satellite angular acceleration which is parallel to their rotational joint axes, i.e.

$$\dot{\boldsymbol{\omega}}_b \parallel \dot{\boldsymbol{\beta}}_{p,i} \tag{3}$$

For the free-floating robot system we assume that the manipulator parameters are known. The parameters to be identified are then defined to be the natural frequency, the mass, the center of mass and the inertia matrix of the satellite base and of the flexible appendages. From these we can determine the relative stiffness and damping matrices.

As a first step, we identify the natural frequency with the use of the measured joint torque sensor signals as well as the satellite base angular velocity signal (gyros). Note that the joint torque sensor is assumed to be after the joint gear, such that we can measure the acting torque without joint friction. Then, applying a Fast Fourier Transformation (FFT) to these signals, the natural frequency can be obtained. The remaining parameters are identified through the formulation of a nonlinear optimization, in which the cost function is defined as the squared sum of the differences between the expected and the measured torques.

Sloshing— In this work, we used a pendulum analogy to model the sloshing effects. In Fig. 31 the principle of the used fuel sloshing model is shown. The model consists of two parts: one fixed mass and one or more slosh masses connected to pendulum, spring and damper elements. The fixed mass m_0 is assumed to be non-sloshing and stationary with respect to the tank and affects the total mass and inertia of the satellite. The second part represents the moving sloshing part of the fluid m_s. The spring and damper elements account for effects caused by viscous and friction forces with the tank walls and forces caused by a diaphragm, typically used in pressurized fuel tanks. The pendulum arm is assumed to be massless. The fulcrum of the pendulum is free to rotate in three dimensions like a spherical joint. Furthermore, in this simplified model it is assumed that the sloshing is only a surface wave. In Fig. 31 a free surface is sketched without any diaphragm. Finally, the initial pendulum deflection α is assumed to be zero without external disturbance.

In this modelling approach, one pendulum represents one sloshing mode. We want to consider only the first fundamental sloshing mode which is assumed to be dominant in

this case. As such only one pendulum is necessary. The resulting equations of motion can be easily set up (similar to the flexible case) and are not repeated here [37].

Similar as in the identification of flexible appendages, we assume that the manipulator inertial model is known. The parameters for the sloshing model to be estimated are defined here as the natural frequency, the mass, the center of mass and the inertia matrix of the satellite base and of the sloshing mass. Furthermore, relative to the pendulum, we ideintify the pendulum length, as well as the spring and damping constants. For the method of identification we apply the same as for the flexible appendages case.

Results— To investigate the performance of the described methods, numerical simulations were conducted both for the flexible model and the liquid sloshing model. For the simulation we used a 7-DoF redundant manipulator mounted on a base satellite with the total manipulator kinematics length of $l_m = 3\ m$. As flexible appendages we defined two solar panels consisting each of two flexible joints, resulting in a total of 4 flexible joints. In this simulation the natural frequency ω_n was estimated out of the joint torque and base velocity data with the Fast Fourier Transformation data of the signals. The generated Power Spectral Density (PSD) of the signals are plotted in Fig. 32. The first two natural frequencies of the flexible free-floating robot system can be seen in the two peaks of the data plot A) and can be quantified with $\omega_{n,1} = 0.23Hz$ and $\omega_{n,2} = 0.68Hz$. The frequencies for the flexible excitation are spread almost equally (see B), whereas the trajectory for the rigid body identification shows a distinct concentration below the critical natural frequencies (C). For the sloshing model, we used one point mass with a 2 DoF joint connected to the fulcrum of the pendulum. The

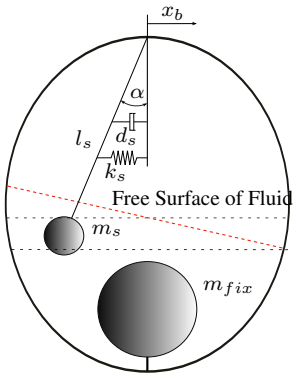

Figure 31: Dynamic model of fuel sloshing - the pendulum equivalent model.

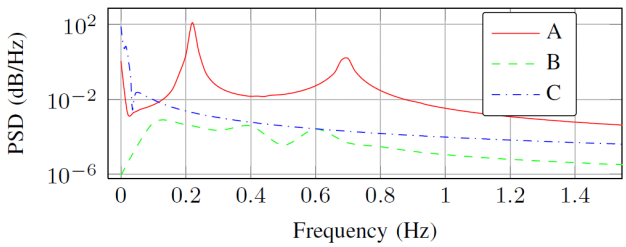

Figure 32: Power Spectral Density (PSD) of A) answer of the flexible appendages, B) excitation trajectory for flexible modes, C) excitation trajectory for rigid body identification.

simulation results of the sloshing model were similar to that of the flexible appendages model. The natural frequency here was calculated to a value of $\omega_n = 0.06Hz$.

7. Conclusion

Different methods were presented which support robotic operations in Low Earth orbit, specifically to accomplish the task of grasping a non-cooperative tumbling target satellite. Both the teleoperation and the autonomous operational modes were addressed. Dedicated functionalities were described and partly validated in simulation and through experimental facilities. The extent of this work shows that these approaches not only provide alternative and powerful solutions to the addressed grasping task, but also that their maturity is sufficient for an orbital demonstration mission.

Acknowledgments

The authors thank the Bavarian Research Foundation for funding this project. We also thank Dr. T. Boge for his kind support with all activities related to the EPOS facility at GSOC (DLR).

References

[1] B. Siciliano and O. Khatib, Eds., *Springer Handbook of Robotics*. Berlin, Heidelberg: Springer, Chapter 45, 2008. [Online]. Available: http://dx.doi.org/10.1007/978-3-540-30301-5

[2] A. Albu-Schäffer, W. Bertleff, D. Rebele, B. Schäfer, K. Landzettel, and G. Hirzinger, "Rokviss - robotics component verification on iss current experimental results on parameter identification," in *ICRA 2006*, May 2006, pp. 3879–3885.

[3] E. Stoll, J. Artigas, J. Letschnik, C. Preusche, U. Walter, and G. Hirzinger, "Ground verification of the feasibility of telepresent on-orbit servicing," *Journal of Field Robotics*, 2008.

[4] J. Ryu, J. Artigas, and C. Preusche, "A passive bilateral control scheme for a teleoperator with time-varying communication delay," *Elsevier Journal of Mechatronics*, vol. 20, pp. 812–823, October 2010.

[5] J. Artigas, J.-H. Ryu, C. Preusche, and G. Hirzinger, "Network representation and passivity of delayed teleoperation systems," in *IROS 2011*, Sept 2011, pp. 177–183.

[6] J. Artigas, J. Ryu, and C. Preusche, "Time domain passivity control for position-position teleoperation architectures," *Presence: Teleoperators and Virtual Environments*, vol. 19, no. 5, pp. 482–497, 2010. [Online]. Available: http://www.mitpressjournals.org/doi/abs/10.1162/pres_a_00013

[7] J. Artigas, "Time domain passivity control for delayed teleoperation," Ph.D. dissertation, Technical University of Madrid (UPM), July 2014.

[8] "SENSODRIVE GmbH," *www.sensodrive.de/EN/*.

[9] A. Fleischner and M. Wilde, "Racoon - a hardware-in-the-loop simulation environment for teleoperated proximity operations," in *Proceedings of the International Symposium on Artificial Intelligence, Robotics and Automation in Space*, ESA, Ed., 2012.

[10] N. W. Oumer and G. Panin, "3d point tracking and pose estimation of a space object using stereo images," in *21st International Conference on Pattern Recognition*, Tsukuba, Japan, Nov 2012, pp. 796–800.

[11] J. M. Kelsey, J. Byrne, M. Cosgrove, S. Seereeram, and R. K. Mehra, "Vision-based relative pose estimation for autonomous rendezvous and docking," in *IEEE Aerospace Conference*, 2006.

[12] C.Miravet, L. Pascual, E. Krouch, and J. Delcura, "An image-based sensor system for autonmous rendez-vous with uncooperative satellites," in *7th International ESA Conference on Guidance, Navigation and Control Systems*, June 2008.

[13] A. Petit, E. March, and K. Kanani, "Vision-based space autonomous rendezvous : A case study," in *IROS 2011*, 2011, pp. 619–624.

[14] N. W. Oumer, "Monocular 3d pose tracking of a specular object," in *Proceedings of the 9th International Conference on Computer Vision Theory and Applications*, vol. 3, 2014, pp. 458–465.

[15] T. Drummond and R. Cipolla, "Real-time visual tracking of complex structures," *IEEE Trans. Pattern Anal. Mach. Intell.*, pp. 932–946, 2002.

[16] A. I. Comport, E. Marchand, and F. Chaumette, "Robust model-based tracking for robot vision," in *IROS 2004*, vol. 1, 2004, pp. 692–697.

[17] T. Boge, T. Wimmer, O. Ma, and T. Tzschichholz, "Epos- using robotics for rvd simulation of on-orbit servicing missions," in *AIAA Modeling and Simulation Technologies Conference, Toronto, Ontario Canada,*, August 2010.

[18] T. Ringbeck, "A 3D time of flight camera for object detection," in *Optical 3-D Measurement Techniques*, 2007.

[19] T. Tzschichholz and K. Schilling, "Range extension of the PMD sensor with regard to applications in space," in *19th IFAC Symposium on Automatic Control in Aerospace*, 2013.

[20] L. Regoli, C. Herrmann, K. Ravandoor, and K. Schilling, "New testing facility for proximity operations in space," in *19th IFAC Symposium on Automatic Control in Aerospace*, 2013.

[21] L. Regoli, K. Ravandoor, M. Schmidt, and K. Schilling, "Advanced techniques for spacecraft motion estimation using PMD sensors," in *1st IFAC conference on Embedded Systems, Computational Intelligence and Telematics in Control*, 2012.

[22] L. Regoli, K. Ravandoor, M.Schmidt, and K. Schilling, "On-line robust pose estimation for rendezvous and docking in space using photonic mixer devices," in *63rd International Astronautical Congress*, 2012.

[23] L. Regoli, K. Ravandoor, M.Schmidt, and K.Schilling, "On-line robust pose estimation for rendezvous and docking in space using photonic mixer devices," *Acta Astronautica*, vol. 96, pp. 159–165, March-April 2014.

[24] K. Ravandoor, S. Busch, L. Regoli, and K. Schilling, "Evaluation and performance optimization of PMD camera for rvd application," in *19th IFAC Symposium on Automatic Control in Aerospace*, 2013.

[25] U. Hillenbrand and R. Lampariello, "Motion and parameter estimation of a free-floating space object from range data for motion prediction," in *Proc. Int. Symp. on Artificial Intelligence, Robotics and Automation in Space (iSAIRAS)*, September 2005.

[26] R. Lampariello, "On grasping a tumbling debris object with a free-flying robot (invited paper)," in *19th IFAC Symposium on Automatic Control in Aerospace, Würzburg, Germany*, September 2013.

[27] R. Lampariello and G. Hirzinger, "Generating feasible trajectories for autonomous on-orbit grasping of spinning debris in a useful time," in *IROS 2013*, Nov 2013.

[28] F. Aghili, "A prediction and motion-planning scheme for visually guided robotic capturing of free-floating tumbling objects with uncertain dynamics." *IEEE Trans. on Robotics*, vol. 28, no. 3, pp. 634–649, 2012.

[29] K. P. Ou Ma, Angel Flores-Abad, "Control of a space robot for capturing a tumbling object," in *Proc. Int. Symp. on Artificial Intelligence, Robotics and Automation in Space (iSAIRAS)*, Sept. 2012.

[30] W. H. Clohessy and R. S. Wiltshire, "Terminal guidance system for satellite rendezvous," *Journal of the Astronautical Sciences*, vol. 27, no. 9, pp. 653–658, 1960.

[31] J. Tschauner and P. Hempel, "Optimale beschleunigungsprogramme für das rendezvous-manöver," *Astronautica Acta*, vol. 10, pp. 296–307, November 1964.

[32] K. Yamanaka and F. Ankersen, "New state transition matrix for relative motion on an arbitrary elliptical orbit," *Journal of Guidance, Control, and Dynamics*, vol. 25, no. 1, pp. 60–66, January 2002.

[33] J. Scharnagl, L. Regoli, and K. Schilling, "On-line collision detection in space using photonic mixer devices," in *19th IFAC Symposium on Automatic Control in Aerospace*, 2013.

[34] J. Scharnagl, L. Regoli, K. Ravandoor, and K. Schilling, "Pose estimation and collision avoidance for rendezvous and docking in space using photonic mixer devices," in *64th Int. Astronautical Congress*, 2013.

[35] W. Rackl, R. Lampariello, and G. Hirzinger, "Robot excitation trajectories for dynamic parameter estimation using optimized b-splines," in *ICRA 2012*, May 2012.

[36] W. Rackl, R. Lampariello, and A. Albu-Schäffer, "Parameter identification methods for free-floating space robots with direct torque sensing," in *19th IFAC Symposium on Automatic Control in Aerospace, Würzburg, Germany*, September 2013.

[37] W. Rackl and R. Lampariello, "Parameter identification of free-floating robots with flexible appendages and fuel sloshing," in *accepted for 6th International Conference on Modelling, Identification and Control, Melbourne, Australia*, December 2014.

BIOGRAPHY

Roberto Lampariello *received his bachelor's degree in aerospace engineering from Southampton University in 1990, master's degree in aeroplane aerodynamics from Cranfield University in 1991 and a specialization degree in aerospace engineering from the University of Rome "La Sapienza" in 1998. He is since then employed as a researcher with the Robotics and Mechatronics Center of the DLR in Germany, where he works in the*

fields of dynamics and control of free-flying space robots and in robot motion planning. Since 2012 he is lecturer at the Chair for Aerospace Engineering of the Technical University in Munich, for a course in orbital and robotic dynamics and control.

Nassir W. Oumer *received Master's degree in Electrical Engineering from Indian Institute of Technology Madras in 2006, Master's degree in Space Technology from the Lulea University of Technology, and Space Robotics and Automation from Helsinki University of Technology with distinction in 2009. He conducted his Master Thesis research on the dynamic modeling and control of Spherical robot. Since 2010, as a research fellow and a doctoral researcher, he has been involved in various On-orbit Servicing Projects at DLR, developing vision-based methods for rendezvous and capture of a satellite. Currently he is also pursuing his PhD at the Faculty of informatics at Technical University of Munich in Computer Vision. His responsibilities as a doctoral candidate include the research and development of vision-based 3D tracking methods for rendezvous and capture of a satellite.*

Dr. Jordi Artigas *is a senior researcher at the Robotics and Mechatronics Center of the DLR - German Aerospace Center and is holder of the European chair of the IEEE Telerobotics Technical Committee. He is coordinator of the euRobotics Topic Group Telerobotics and Teleoperation. Jordi holds a Master degree in electrical engineering from the Universtitat Ramon Llull (Barcelona) and a Ph.D. in robotics, control and automation from the Technical University of Madrid (UPM). In his Ph.D., Jordi proposed a new framework to design bilateral control architectures using delayed communications and data losses based on the passivity criteria. This framework has been already used in space robotics missions. He is currently coordinating the DLR On-Orbit Servicing hardware simulator (DEOS-SIM), composed of two free-floating satellites and a servicer robotic arm.*

Wolfgang Rackl *studied Mechanical Engineering at the Technische Hochschule Ingolstadt and at the Royal Melbourne Institute of Technology (RMIT), Australia, and received a Bachelor's degree (Dipl.-Ing. (FH)) in 2005 and a Master's degree in Aerospace Engineering from the Technical University Munich (TUM) in 2009. He conducted his Master Thesis research in detumbling strategies for On-Orbit Servicing missions. Since 2009 he is pursuing his PhD at the Institute of Robotics and Mechatronics at German Aerospace Center (DLR) in the field of space robotics. His responsibilities as a research associate at the institute include dynamics modelling, parameter identification and contributing to the On-Orbit Servicing experimental verification platform at the institute.*

Dr. Giorgio Panin *received the Master degree in electrical engineering (1998), and the PhD in robotics (2002) from the University of Genoa (Italy), Chair of robotics and embedded systems. From 2002 to 2010, he has been a post-Doc and Assistant Professor in computer vision at the Informatics faculty of the Technical University of Munich (TUM), where he developed model-based object tracking methods in the context of national (DFG) and EU-funded projects. During this time he published a book, co-authored several conference and journal papers, and received in 2011 the German degree for University teaching (Habilitation). Subsequently, he joined as a research assistant the German Aerospace Center (DLR), Institute of Robotics and Mechatronics, where he is presently involved in visual tracking for on-orbit servicing.*

Dr. Jan Harder *received his diploma of Mechanical Engineering from the Technical University Munich in 2008. Since then he worked as a research assistant at the institute of astronautics at the Technical University Munich focusing on satellite technologies for real-time applications. After working in a satellite antenna development project he started his doctoral studies about real-time communication architectures and the characterization of communication links for tele-operated spacecraft.*

Ralf Purschke *received a Master's degree in Aerospace Engineering from the Technical University Munich (TUM) in 2009. As a graduate student he was involved in designing an experiment for the sounding rocket REXUS, and in the CubeSat project MOVE where he was responsible for the structures subsystem. He conducted his Master Thesis research at the University of Colorado in Boulder on the body posture of astronauts in microgravity. Since 2009 he is pursuing his PhD at the Institute of Astronautics at TUM in space mechanisms. His responsibilities as a research associate at the institute included the design, manufacture and test of an Antenna Pointing Mechanism for a Ka-band antenna.*

Professor Dr. Ulrich Walter *is the head of the Institute of Astronautics at Technical University Munich. He received his Ph.D. in nuclear physics at the University of Cologne. Afterwards he spent two years pursuing post-doctoral studies at Argonne National Laboratory and Berkeley before he was selected for the German Astronautics program. He flew aboard Space Shuttle Columbia in the 1993 Spacelab D2 mission. After working at the German Aerospace Center (DLR) and IBM, he received a call to LRT in 2003. His research interest is the development of enabling technologies for future satellite systems, with a focus on teleoperation technologies for On-Orbit Servicing and space debris removal.*

Jürgen Frickel *received a Master's degree in Electrical, Electronic and Communication Engineering (EEI) from the Friedrich-Alexander-Universität Erlangen -Nürnberg (FAU) in 1986. Since 1987 he has held different positions at FAU and was involved in research and education in microelectronics and the design of integrated circuits, especially for digital design methods. Since 2005 his interests are more focused on the design of robust circuits and systems for ground and space applications. In the Department of EEI, Information Technology he offers courses in the fields of digital design methods, hardware description languages and communication structures.*

Ismar Masic *received his Diploma Degree in Electrical Engineering from the University Duisburg-Essen in 2007. After joining SpaceTech GmbH in 2008 he worked in the area of satellite dynamics simulation. Within the project DEOS, phase B1 he was responsible for the attitude determination and control analyses of the Client satellite. Later he worked on algorithms for performance improvement of an earth and sun sensor. In FORROST he developed a radiometric camera simulator. Currently he is working on the development of a miniaturized animal tracking device for the ICARUS mission.*

Karthik Ravandoor *received his B.E. in Computer Science and Engineering from Bangalore University, India in 2000 and M.Sc. degrees in Space Science and Technology from University of Würzburg and Luleå University of Technology in 2003. He is currently working as a PhD student and research assistant at the department of Robotics and Telematics in University of Würzburg. His current research interests include range sensors for space applications, spacecraft formation flying and relative navigation for On-orbit servicing.*

Julian Scharnagl *received a bachelor degree in Physics from University of Würzburg in 2010. He continued his studies in the joint European master program in Space Science and Technology at University of Würzburg and Luleå University of Technology and conducted his master thesis on 3D vision-based collision detection for rendezvous and docking in space. He finished his master degree in 2012 and since 2013 he is a PhD student and research assistant at the Robotics and Telematics chair at University of Würzburg. His field of work include close range maneuver in space, vision-based relative navigation as well as formation flying.*

Professor Dr. Klaus Schilling *is chair for Robotics and Telematics at the Julius-Maximilian-University Würzburg and President of the research company "Center for Telematics". Earlier he worked in space industry on system design of interplanetary satellites and vehicles (Huygens, Rosetta, Mars Rovers). Current research emphasis is on control aspects of autonomous and teleoperated systems, as well as on pico-satellites. His team developed the first German pico-satellite UWE-1. He was Chairman of the IFAC Technical Committee on Aerospace, is member of its steering committee and was selected as member of the International Academy of Astronautics.*

Klaus Landzettel *received a Dipl.-Ing. degree in telecommunication and high frequency technique from the Fachhochschule Darmstadt, Germany, in 1970.Since 1970 he has been with the Institute of Robotics and Mechatronics, German Aerospace Centre (DLR), Weling, Germany. He has a strong experience in space robotics. In ROTEX he was responsible for co-ordination of the software development for the on-board and on-ground systems, the performance of the astronaut's payload training, and operation of the onboard robot from the ground station during the D2 mission. He was managing many national and international space projects like the German / Japanese project GETEX / ETS VII, VENUS, MARCO, ESS, ESS-T, VITAL, CIRCUS, AROMA, ROKVISS, DEOS to name a few. In 2005 he was awarded with the "Goldene Wernher von Braun Medaille" and in 2011 as DLR Senior Scientist.*

Professor Dr. Gerd Hirzinger *received his Dipl.-Ing. Degree 1969 and the doctor's degree 1974 from the Technical University of Munich. In 1969 he joined DLR (German Aerospace Center) where he became head of the automation and robotics laboratory in 1976. In 1991 he received a joint professorship from the Technical University of Munich. Since 1992 he has been director at DLR's Institute of Robotics and Mechatronics, which is one of the biggest and most acknowledged centers in the field worldwide, including not only robot development for space and terrestrial applications, but also aircraft control and optimization, vehicle technology (including electro mobility) and medical technology (artificial hearts and surgical robots). He has published more than 600 papers in robotics, mainly on robot sensing, sensory feedback, mechatronics, man-machine interfaces, telerobotics and space robotics. And he has received numerous high-ranked national and international awards.*